Cerebral Cortex, July 2016;26: 2937–2951

doi: 10.1093/cercor/bhv032
Advance Access Publication Date: 17 June 2015
Original Article

ORIGINAL ARTICLE

Cdk5 is a New Rapid Synaptic Homeostasis Regulator Capable of Initiating the Early Alzheimer-Like Pathology

Yanghui Sheng[1,2,4,†], Lei Zhang[1,†], Susan C. Su[3], Li-Huei Tsai[3], and J. Julius Zhu[1]

[1]Department of Pharmacology, University of Virginia School of Medicine, Charlottesville, VA 22908, USA, [2]Undergraduate Class of 2011, Yuanpei Honors College, Peking University, Beijing 100871, China, [3]Picower Institute for Learning and Memory and Howard Hughes Medical Institute, Massachusetts Institute of Technology, Cambridge, MA 02139, USA, and [4]Current address: Department of Neuroscience, Johns Hopkins University School of Medicine, Baltimore, MD 21205, USA

Address correspondence to J. Julius Zhu, Department of Pharmacology, University of Virginia School of Medicine, 1300 Jefferson Park Avenue, Charlottesville, VA 22908, USA. Email: jjzhu@virginia.edu

[†]These authors contributed equally.

Abstract

Cyclin-dependent kinase 5 (Cdk5) is a serine/threonine kinase implicated in synaptic plasticity, behavior, and cognition, yet its synaptic function remains poorly understood. Here, we report that physiological Cdk5 signaling in rat hippocampal CA1 neurons regulates homeostatic synaptic transmission using an unexpectedly rapid mechanism that is different from all known slow homeostatic regulators, such as beta amyloid (Aβ) and activity-regulated cytoskeleton-associated protein (Arc, aka Arg3.1). Interestingly, overproduction of the potent Cdk5 activator p25 reduces synapse density, and dynamically regulates synaptic size by suppressing or enhancing Aβ/Arc production. Moreover, chronic overproduction of p25, seen in Alzheimer's patients, induces initially concurrent reduction in synapse density and increase in synaptic size characteristic of the early Alzheimer-like pathology, and later persistent synapse elimination in intact brains. These results identify Cdk5 as the regulator of a novel rapid form of homeostasis at central synapses and p25 as the first molecule capable of initiating the early Alzheimer's synaptic pathology.

Key words: Cdk5, cortex, hippocampus, neurodegenerative diseases, synaptic depression, synaptic homeostasis

Introduction

Cyclin-dependent kinase 5 (Cdk5) is a serine/threonine kinase highly expressed in the brain (Su and Tsai 2011; Cheung and Ip 2012). The pivotal role of Cdk5 in synaptic plasticity, behavior, and cognition was first implicated by the chronic overproduction of a potent Cdk5 activator, p25, and hyperactivated Cdk5 signaling observed in the brain of Alzheimer's patients (Patrick et al. 1999). The view was strengthened by later studies showing that transgenic mice overexpressing p25 exhibit reduced synaptic plasticity and impaired cognition. These and other relevant findings establish the functional significance of Cdk5 signaling, but also raise an important mechanistic question on how Cdk5 signals synaptic function and malfunction (Su and Tsai 2011; Cheung and Ip 2012). Although subsequent studies have provided more supports for the involvement of Cdk5 signaling at synapses, the exact function of Cdk5 remains elusive. For example, some studies showed that Cdk5 suppresses the N-methyl-D-aspartate (NMDA)-sensitive glutamatergic receptor (-R)-mediated synaptic transmission (Hawasli et al. 2007; Plattner et al. 2014), whereas the others reported that Cdk5 signaled a rapid depression of α-Amino-3-hydroxy-5-methyl-4-isoxazolepropionic acid (AMPA)-R-mediated transmission with a time course of less than an hour, via a presumably rapid kinase mechanism (Chergui et al. 2004; Peng et al. 2013). Moreover, several laboratories independently demonstrated that Cdk5 regulated AMPA-R-mediated transmission using a homeostasis-like mechanism (Seeburg et al. 2008; Kim and Ryan 2010; Mitra et al. 2011), which is

expected to take >2–12 h to occur (Turrigiano 2008). Furthermore, if Cdk5 signaling does rapidly depress synaptic transmission, sustained activation of Ckd5 signaling should suppress the production of slow homeostatic regulators, such as Aβ (Turrigiano 2008). However, 2 studies found that chronic hyperactivation of Cdk5 stimulated production of Aβ (Cruz et al. 2006; Wen et al. 2008). These seemingly paradoxical findings further underscore the importance of clarifying the functional role of CDk5 at synapses.

Unveiling the molecule(s) responsible for the early pathogenesis of Alzheimer's disease is central to developing the early diagnosis and effective treatment for the disorder (DeKosky and Marek 2003; Selkoe 2012). There is now abundant evidence indicating that synapses are the initial targets of Alzheimer's disease (Sheng et al. 2012). In particular, independent groups have reported concurrent reduction in synapse density and increase in synaptic size in brains of patients with Alzheimer's disease, as well as human subjects with subjective and mild cognitive impairments (Davies et al. 1987; Bertoni-Freddari et al. 1990; DeKosky and Scheff 1990; Scheff et al. 2006). Interestingly, the changes in both synapse density and synaptic size correlate with the levels of cognitive impairment in the individuals with subjective-mild cognitive impairment and Alzheimer's disease (DeKosky and Scheff 1990; Scheff and Price 2006; Scheff et al. 2006), indicating an early pathology. Subsequent studies have confirmed the characteristic synaptic pathology in multiple brain areas vulnerable to the disease, including the frontal cortex, temporal cortex, cingulate cortex, hippocampal CA1, and dentate gyrus areas (Scheff and Price 2006; Arendt 2009). Over a century of Alzheimer's research has linked a large number of molecules to progressive synaptic depression and synapse loss (Su and Tsai 2011; Cheung and Ip 2012; Guerreiro et al. 2012; Selkoe 2012), a common pathology shared by various mental, neurological, and psychiatric disorders. Yet, whether any of these molecules may have the capability of inducing the concurrent reduction in synapse density and increase in synaptic size, a characteristic synaptic pathology observed in Alzheimer's brains, has never been investigated.

In this study, we used the high-resolution multiple patch-clamp recordings and electron microscopic techniques to analyze synaptic Cdk5 signaling in the timescales ranging from several minutes to multiple days. We discovered that Cdk5 signaled synaptic homeostatic regulation with an unusually fast feedback mechanism; Cdk5 was rapidly activated by synaptic activity within ~15 min, and in turn quickly depressed synaptic transmission within ~30 min. Interestingly, the unique rapid signaling kinetics rendered Cdk5, when chronically stimulated by p25, capable of dynamically regulating the production of slow homeostatic regulators, such as Aβ and Arc. As a consequence, chronic overproduction of p25 induced initially concurrent reduction in synapse density and increase in synaptic size by simultaneously enhancing Cdk5 signaling and suppressing Aβ/Arc signaling, and later, persistent synapse elimination by stimulating both Cdk5 and Aβ/Arc signaling. Our results indicate that Cdk5 regulates a novel rapid form of homeostasis at central synapses and that p25 is the first molecule capable of initiating the characteristic early Alzheimer-like synaptic pathology.

Materials and Methods

Biochemical Analysis

Cultured slices were prepared from postnatal 6–7-day-old male and female rats following previously reported procedure (Qin et al. 2005; Myers et al. 2012; Lim et al. 2014). All procedures for animal surgery and maintenance were performed following protocols approved by the Animal Care & Use Committee of the University of Virginia (Protocol No. 3168) and in accordance with US National Institutes of Health guidelines. Hippocampal extracts were prepared by homogenizing rat hippocampal CA1 regions isolated from hippocampal cultured slices or cells. To reduce the variance and increase the detection resolution, the control and experimental tests were typically carried out using the same sets of cultured slices, the hippocampal CA1 cell lysates were simultaneously collected and processed, and the protein concentration of the lysates was measured and normalized with a spectrophotometer (Shimadzu). The expression levels of endogenous and recombinant Cdk5 in CA1 neurons were estimated taking into account the expression in nonpyramidal neurons (see Supplementary Fig. S1). Cdk5 kinase activity was measured using a previously established Cdk5 kinase activity assay (Tsai et al. 1993; Sharma et al. 1999; Liu et al. 2001). Briefly, Cdk5 immunoprecipitated by mouse anti-Cdk5 (Millipore) was incubated at 4°C with histone H1 and magnesium/ATP mixture at 30°C for 30 min. The phosphorylated rabbit histone H1 was then blotted with specific antiphospho-histone H1 antibody (1:1000; Millipore). Cdk5, Aβ, Arc, and tubulin were blotted using rabbit anti-Cdk5 (1:1000; Millipore), anti-Aβ (1:4000; Abcam), anti-Arc (1:10 000; Millipore), and antitubulin (1:5000; Cell Signaling). Western blots were quantified by chemiluminescence and densitometric scanning of the films under linear exposure conditions. Released Aβ in the culture media collected daily was measured using the rat Aβ (1–40) ELISA kit (Wako) and rat Aβ (1–42) ELISA kit, high sensitive (Wako).

Constructs of Recombinant Proteins and Expression

Cdk5 mutant constructs, as well as p25 and p35 (Patrick et al. 1999; Seo et al. 2014), were subcloned into pEGFP-C1 (enhanced green fluorescent protein [GFP]; Clontech) and/or pC/RFP-C1 (CFP and mCherry were gifts from R. Tsien). In some experiments, RFP or GFP was coexpressed with p25 or amyloid precursor protein (APP) using an internal ribosomal entry site sequence pCITE-RFP or pCITE-GFP. The tagged Cdk5, p25, p35, and APP, as well as GFP and CFP, were then subcloned into Sindbis viral vectors and expressed in CA1 neurons in cultured hippocampal slices or intact brains for a period of 18 ± 1 h to 7 days following previous studies (Qin et al. 2005; Hu et al. 2008). Cdk5-targeting shRNAs and control constructs were subcloned into a lentiviral vector and expressed in CA1 neurons in cultured hippocampal slices for 66 ± 6 h. To increase infection efficiency and reduce toxicity, viruses were filtered with a 0.45 μm PVDF filter (Millipore) and used within 2 weeks after preparation. The knockdown efficiencies of 4 shRNAs that target different Cdk5 sequences were assessed using cultured hippocampal neurons, and 2 effective shRNAs and their control scrambled constructs were chosen to use in this study. Expression of Rap1 and/or Rap2 mutants was achieved using biolistic transfection for 18–20 h. For in vitro expression, neurons were infected or transfected after 6–14 days in culture. For in vivo expression, P14–20 male and female rats were initially anesthetized by an intraperitoneal injection of ketamine and xylazine (10 and 2 mg/kg, respectively), then placed in a stereotaxic frame with a hole of ~1 × 1 mm drilled above the right barrel cortex. A glass pipette was used to penetrate into the hippocampus according to stereotaxic coordinates and ~50 nL of viral solution was delivered by pressure injection.

Electron Microscopy

Electron microscopic examination of synapses followed methods from previous studies (Kielland et al. 2009; Jiang et al. 2013;

Lee et al. 2015). In brief, for in vivo preparation, rats were anesthetized by an intraperitoneal injection of ketamine and xylazine and then intracardially perfused with freshly prepared 3% acrolein/2% paraformaldehyde in 0.1 M phosphate buffered saline (PBS). The brain blocks containing the hippocampus were removed, postfixed for 2 h in 2% paraformaldehyde, and sectioned at 60 μm. For in vitro preparation, cultured slices were fixed in freshly prepared 3% acrolein/4% paraformaldehyde in 0.1 M PBS at room temperature overnight, and sectioned into 60 μm slices. With high-titer viruses, >80% of CA1 neurons in intact brains and >99% of CA1 neurons in cultured slices, identified by C/G/RFP fluorescence and/or C/G/RFP immunostaining, were infected near the injection sites. The highly infected CA1 stratum radiatum regions were then excised (from the same slices if examined with fluorescence or neighboring slices if examined with immunostaining) and resectioned into 80 nm ultrathin sections using an ultramicrotome. Ultrathin sections were examined with a transmission electron microscope (JEOL-1010; Japan Electron Optic, Tokyo, Japan). Synapses were defined by the presence of a clear postsynaptic density (PSD) facing a presynaptic structure with synaptic vesicles. Synapse density was quantified by counting synapses in 10 × 10 μm ultrathin sections and synaptic size was determined by measuring the length of their PSDs.

Electrophysiology

Simultaneous multiple whole-cell recordings were obtained from pairs, triplets, or quadruplets of nearby infected and noninfected CA1 neurons (Zhu et al. 2005; Jiang et al. 2013), under visual guidance using fluorescence and transmitted light illumination, using up to 4 Axopatch-200B or Axoclamp 2B amplifiers (Axon Instruments, Foster City, CA). Bath solution (29 ± 1.5°C), unless otherwise stated, contained (in mM): NaCl 119, KCl 2.5, $CaCl_2$ 4, $MgCl_2$ 4, $NaHCO_3$ 26, NaH_2PO_4 1, glucose 11, picrotoxin (PTX) 0.1, bicuculline 0.01, and 2-chloroadenosine 0.002, at pH 7.4 and gassed with 5% CO_2/95% O_2. 2-chloroadenosine was included to prevent bursting and PTX was excluded when γ-aminobutyric acid (GABA) responses were examined. 2-chloroadenosine was excluded and 2 μM tetrodotoxin (TTX) was included when miniature excitatory postsynaptic currents (mEPSCs) were studied. For experiments in which slices were maintained in culture with additional 10 mM Mg^{2+}, 2 μM TTX, 20 μM PTX, 5 μM SP600125, 2 μM SB203580, 100 μM DL-APV, and/or 5 μM 5,7-dichlorokynurenic acid (DCKA), these chemicals and/or compounds were included at the time of viral infection and removed during recordings. Patch recording pipettes (3–6 MΩ) for current (voltage-clamp) recordings contained (in mM): cesium methanesulfonate 115, CsCl 20, HEPES 10, $MgCl_2$ 2.5, Na_2ATP 4, Na_3GTP 0.4, sodium phosphocreatine 10, EGTA 0.6, and spermine 0.1, at pH 7.25; and for voltage (current-clamp) recordings contained: potassium gluconate 115, HEPES 10, $MgCl_2$ 2, MgATP 2, Na_2ATP 2, Na_3GTP 0.3 and KCl 20, at pH 7.25. Synaptic responses were evoked by bipolar electrodes with single voltage pulses (200 μs, up to 20 V) placed in the stratum radiatum ~300–500 μm away from the CA1 cells. Synaptic AMPA and NMDA responses at −60 and +40 mV were averaged over 90 trials. To minimize the effect from AMPA responses, the peak NMDA responses at +40 mV were measured after digital subtraction of estimated AMPA responses at +40 mV. Quadruple recordings from CFP-, p25-, APP-expressing and nonexpressing neurons were made from CA1 neurons >50 μm apart to avoid the effects resulting from diffused Aβ (Wei et al. 2010). To ensure the detection of the smallest synaptic events, mEPSCs were analyzed using only the high-quality patch-clamp recordings with the low baseline noise (≤2 pA) obtained by gently breaking-in high-resistance seal (>10 GΩ) patches (Wang et al. 2015). Synaptic plasticity experiments followed our previous reports (Zhu et al. 2002, 2005; McCormack et al. 2006). Briefly, long-term potentiation (LTP) was induced by a pairing protocol using 200 pulses at 2 Hz at −5 mV within 5 min after formation of whole-cell configuration. Depotentiation was induced by a pairing protocol using 300 pulses at 1 Hz at −45 mV 30 min after induction of LTP in the presence of SB203580, which blocks long-term depression (LTD). To examine the strength of Aβ/Arc signaling that mediates LTD and avoid inducing the saturated LTD, submaximal LTD stimuli (i.e., 200 pairing pulses at 1 Hz at −45 mV; cf. McCormack et al. 2006) were delivered 15 min after formation of whole-cell configuration. Slices were incubated in solution containing 5 μM SP600125 and 2 μM SB203580 before (for at least 1 h) and during LTP and LTD in some experiments, respectively. Because no difference in LTP was found in neurons recorded with the whole-cell and perforated-patch recording techniques (see Supplementary Table S1), the data were pooled together in analysis. Sindbis viral expression system produced the rapid overexpression of recombinant proteins, including Cdk5 (see Supplementary Fig. S1), p25 and p35 (Ctrl: 100.0 ± 5.9%; p25: 405.4 ± 21.6%; $n = 12$; $P < 0.005$; p35: 381.9 ± 18.2%; $n = 12$; $P < 0.005$). The levels of overexpression of p25 were comparable with the high end of p25 overproduction observed in Alzheimer's patients (Patrick et al. 1999; Tseng et al. 2002; Swatton et al. 2004). Correspondingly, p25-expressing rat neurons exhibited the concurrent reduction in synapse density and increase in synaptic size for ~7 days, equivalent to ~1–1.5 human years or the minimal time required for the conversion from subjective-mild cognitive impairment to Alzheimer's disease in human subjects (DeKosky and Marek 2003; Scheff et al. 2006; Reisberg et al. 2010). Approximately 5–15% neurons began to show signs of deterioration after Sindbis viral expression of recombinant proteins for >7 days; they display reduced input resistance (< 100 MΩ), increased holding current (>200 pA at −60 mV), and recordings from these neurons were frequently lost within ~5 min. Therefore, to avoid the nonspecific effects, all experiments, including the control GFP- or CFP-alone expression experiments, were performed within 7 days after expression of recombinant proteins.

Statistical Analysis

Statistical results were reported as mean ± SEM. Statistical significances of the means ($P \leq 0.05$; 2 sides) were determined using Wilcoxon and Mann–Whitney Rank Sum nonparametric tests for paired and unpaired samples, respectively.

Results

Cdk5 Signals a Novel Rapid Synaptic Homeostasis

To investigate the synaptic function of Cdk5 signaling, we acutely expressed a series of GFP-tagged constructs designed to modulate Cdk5 signaling in hippocampal CA1 neurons in cultured slices (Fig. 1A). Western blot analysis showed that ~18 h after infection, the expression levels of Cdk5-GFP ranged from ~3–4 times the endogenous Cdk5 level in CA1 neurons (see Supplementary Fig. S1). We then made simultaneous electrophysiological recordings from nearby nonexpressing CA1 neurons and CA1 neurons expressing the GFP-tagged physiological activators of Cdk5, including both the long-lasting activator p25 (p25-GFP) and short-lasting activator p35 protein (p35-GFP) (Su and Tsai 2011; Cheung and Ip 2012). Afferent fibers were stimulated and

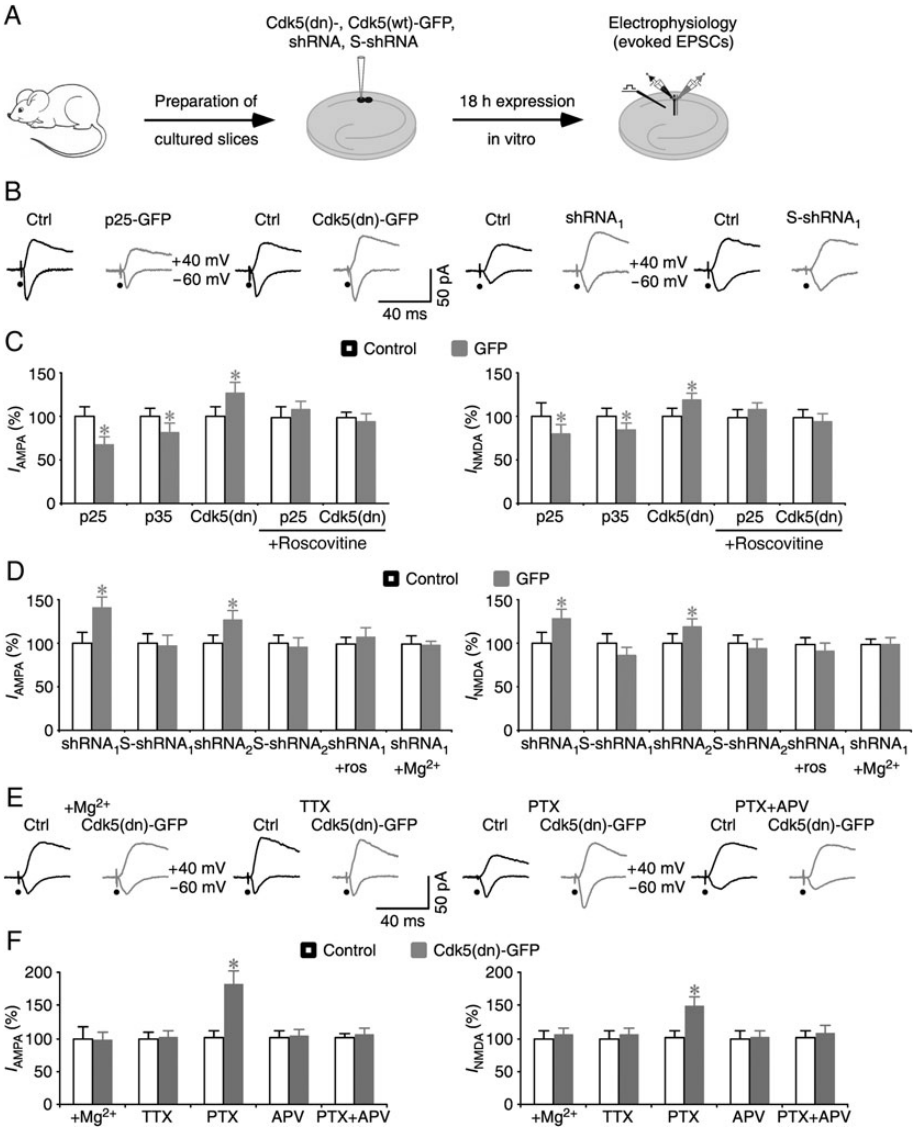

Figure 1. Cdk5 regulates homeostasis of glutamatergic synaptic transmission. (*A*) Schematic drawing outlines in vitro experimental design. (*B*) Evoked AMPA-R- (−60 mV) and NMDA-R- (+40 mV) mediated responses recorded from neighboring nonexpressing (Ctrl) and p25-GFP, Cdk5(dn)-GFP, $shRNA_1$, or S-$shRNA_1$ expressing cells in normal media. (*C*) AMPA and NMDA responses in expressing neurons relative to neighboring nonexpressing control cells. Values for AMPA responses in neurons expressing p25-GFP (Ctrl: −36.1 ± 3.9 pA; Exp: −24.0 ± 3.7 pA; $n = 22$; $P < 0.01$), p35-GFP (Ctrl: −35.6 ± 3.3 pA; Exp: −29.2 ± 3.5 pA; $n = 26$; $P < 0.005$), Cdk5(dn)-GFP (Ctrl: −33.8 ± 3.5 pA; Exp: −42.9 ± 4.1 pA; $n = 30$; $P < 0.005$), p25-GFP with 25 μM roscovitine in culture media (Ctrl: −32.6 ± 4.0 pA; Exp: −35.4 ± 3.3 pA; $n = 22$; $P = 0.64$), and Cdk5(dn)-GFP with 25 μM roscovitine in culture media (Ctrl: −38.8 ± 2.4 pA; Exp: −37.0 ± 3.6 pA; $n = 26$; $P = 0.73$). Values for NMDA responses in neurons expressing p25-GFP (Ctrl: 48.5 ± 7.9 pA; Exp: 38.9 ± 5.3 pA; $n = 22$; $P < 0.05$), p35-GFP (Ctrl: 65.5 ± 6.3 pA; Exp: 55.3 ± 5.2 pA; $n = 26$; $P < 0.05$), Cdk5(dn)-GFP (Ctrl: 52.2 ± 5.0 pA; Exp: 61.7 ± 4.7 pA; $n = 30$; $P < 0.005$), p25-GFP with 25 μM roscovitine in culture media (Ctrl: 74.8 ± 6.5 pA; Exp: 81.5 ± 5.9 pA; $n = 22$; $P = 0.37$), and Cdk5(dn)-GFP with 25 μM roscovitine in culture media (Ctrl: 105.2 ± 9.3 pA; Exp: 100.1 ± 8.7 pA; $n = 26$; $P = 0.79$). (*D*) AMPA and NMDA responses in expressing neurons relative to neighboring nonexpressing control cells. Values for AMPA responses in neurons expressing $shRNA_1$ (Ctrl: −11.6 ± 1.5 pA; Exp: −16.3 ± 1.4 pA; $n = 26$; $P < 0.05$), S-$shRNA_1$ (Ctrl: −19.9 ± 2.3 pA; Exp: −19.2 ± 2.5 pA; $n = 24$; $P = 0.84$), $shRNA_2$ (Ctrl: −19.2 ± 1.7 pA; Exp: −24.2 ± 2.3 pA; $n = 28$; $P < 0.05$), S-$shRNA_2$ (Ctrl: −19.9 ± 2.0 pA; Exp: −19.1 ± 2.2 pA; $n = 20$; $P = 0.82$), $shRNA_1$ with 25 μM roscovitine in culture media (Ctrl: −19.9 ± 2.0 pA; Exp: −19.1 ± 2.2 pA; $n = 20$; $P = 0.82$), or $shRNA_1$ with 12 mM Mg^{2+} in culture media (Ctrl: −18.3 ± 1.1 pA; Exp: −17.1 ± 1.6 pA; $n = 26$; $P = 0.23$). Values for NMDA responses in neurons expressing $shRNA_1$ (Ctrl: 32.8 ± 4.3 pA; Exp: 41.9 ± 3.4 pA; $n = 26$; $P < 0.05$), S-$shRNA_1$ (Ctrl: 70.6 ± 7.6 pA; Exp: 61.0 ± 5.8 pA; $n = 24$; $P = 0.38$), $shRNA_2$ (Ctrl: 57.0 ± 6.1 pA; Exp: 67.6 ± 5.7 pA; $n = 28$; $P < 0.05$), and S-$shRNA_2$ (Ctrl: 46.9 ± 4.5 pA; Exp: 43.7 ± 5.2 pA; $n = 20$; $P = 0.79$), $shRNA_1$ with 25 μM roscovitine in culture media (Ctrl: 46.9 ± 4.5 pA; Exp: 43.7 ± 5.2 pA; $n = 20$; $P = 0.79$), or $shRNA_1$ with 12 mM Mg^{2+} in culture media (Ctrl: 40.6 ± 2.6 pA; Exp: 39.1 ± 2.4 pA; $n = 26$; $P = 0.59$). (*E*) Evoked AMPA-R- (−60 mV) and NMDA-R- (+40 mV) mediated responses recorded from neighboring nonexpressing (Ctrl) and Cdk5(dn)-GFP expressing cells in media containing 12 mM Mg^{2+}, 2 μM TTX, 20 μM PTX, or 20 μM PTX and 100 μM DL-APV. (*F*) AMPA and NMDA responses in neurons expressing Cdk5(dn)-GFP relative to neighboring nonexpressing control cells. Values for AMPA responses in Cdk5(dn)-GFP expressing neurons cultured in media with Cdk5(dn)-GFP with 12 mM Mg^{2+} in culture media (Ctrl: −28.5 ± 4.9 pA; Exp: −27.7 ± 3.4 pA; $n = 20$; $P = 0.82$), 2 μM TTX (Ctrl: −32.8 ± 2.9pA; Exp: −33.5 ± 3.2 pA; $n = 24$; $P = 0.61$), 20 μM PTX (Ctrl: −31.3 ± 3.6 pA; Exp: −56.5 ± 6.4 pA; $n = 30$; $P < 0.0005$), 100 μM DL-APV (Ctrl: −32.7 ± 3.4 pA; Exp: −33.9 ± 3.3 pA; $n = 26$; $P = 0.71$), or 20 μM PTX and 100 μM DL-APV (Ctrl: −28.5 ± 1.9 pA; Exp: −30.0 ± 2.7 pA; $n = 26$; $P = 0.59$), and values for NMDA responses in Cdk5(dn)-GFP with 12 mM Mg^{2+} in culture media (Ctrl: 56.0 ± 8.0 pA; Exp: 57.3 ± 6.6 pA; $n = 20$; $P = 0.97$), Cdk5(dn)-GFP expressing neurons cultured in media with 2 μM TTX (Ctrl: 56.0 ± 6.0 pA; Exp: 58.9 ± 6.2 pA; $n = 24$; $P = 0.53$), 20 μM PTX (Ctrl: 52.9 ± 5.6 pA; Exp: 78.2 ± 7.8 pA; $n = 30$; $P < 0.0005$), 100 μM DL-APV (Ctrl: 73.9 ± 8.2 pA; Exp: 75.0 ± 7.3 pA; $n = 26$; $P = 0.83$), or 20 μM PTX and 100 μM DL-APV (Ctrl: 59.7 ± 7.1 pA; Exp: 63.9 ± 7.9 pA; $n = 26$; $P = 0.23$). Note that the relative enhancements of AMPA and NMDA responses in Cdk5(dn)-GFP expressing neurons cultured in media with 20 μM PTX are significantly greater than those cultured in normal media ($P < 0.05$; Mann–Whitney Rank Sum test). AMPA-R- and NMDA-R-mediated current amplitudes and standard errors were normalized to average values from control cells. Asterisks indicate $P < 0.05$ (Wilcoxon tests).

excitatory postsynaptic currents (EPSCs) were recorded. Neurons expressing p25-GFP or p35-GFP showed depressed NMDA-R- and AMPA-R-mediated responses (by ~25–30%) compared with nearby control nonexpressing neurons (Fig. 1*B*,*C*). To test whether endogenous Cdk5 activity depresses transmission, we expressed a dominant negative mutant Cdk5(K33→T), Cdk5(dn)-GFP. Neurons expressing Cdk5(dn)-GFP had increased NMDA and AMPA responses compared with nearby nonexpressing control neurons (Fig. 1*B*,*C*). Previous studies have shown that bath application of roscovitine, a pharmacological inhibitor of Cdk5, inhibits Cdk5 signaling (Tomizawa et al. 2002; Yan et al. 2002). We included roscovitine in culture media during expression of P25-GFP and Cdk5(dn)-GFP. In the presence of roscovitine, neurons expressing P25-GFP or Cdk5(dn)-GFP had the same NMDA and AMPA responses compared with nearby control nonexpressing neurons (Fig. 1*B*,*C*). These results suggest that pharmacological inhibition of endogenous Cdk5 signaling blocked the depression in p25-GFP expressing neurons and occluded the potentiation in Cdk5(dn)-GFP expressing neurons. Expression of p25-GFP and Cdk5(dn)-GFP had no effects on intrinsic membrane properties (i.e., the resting membrane potential, input resistance, and membrane time constant), GABAergic responses and paired pulse facilitation of AMPA responses (see Supplementary Fig. S2). These results suggest that endogenous Cdk5 depresses postsynaptic glutamatergic transmission in CA1 neurons.

To confirm that endogenous Cdk5 depresses glutamatergic transmission, we knocked down endogenous Cdk5 in CA1 neurons using short hairpin interference RNAs (shRNAs), which were delivered along with GFP using a lentivirus. Expression of Cdk5-targeting shRNAs (i.e., $shRNA_1$ and $shRNA_2$) for 60–72 h reduced Cdk5 expression levels in neurons by ~95%, whereas expression of their scrambled controls (i.e., S-$shRNA_1$ and S-$shRNA_2$) had no effect on Cdk5 expression (see Supplementary Fig. S3). Electrophysiological recordings showed that neurons

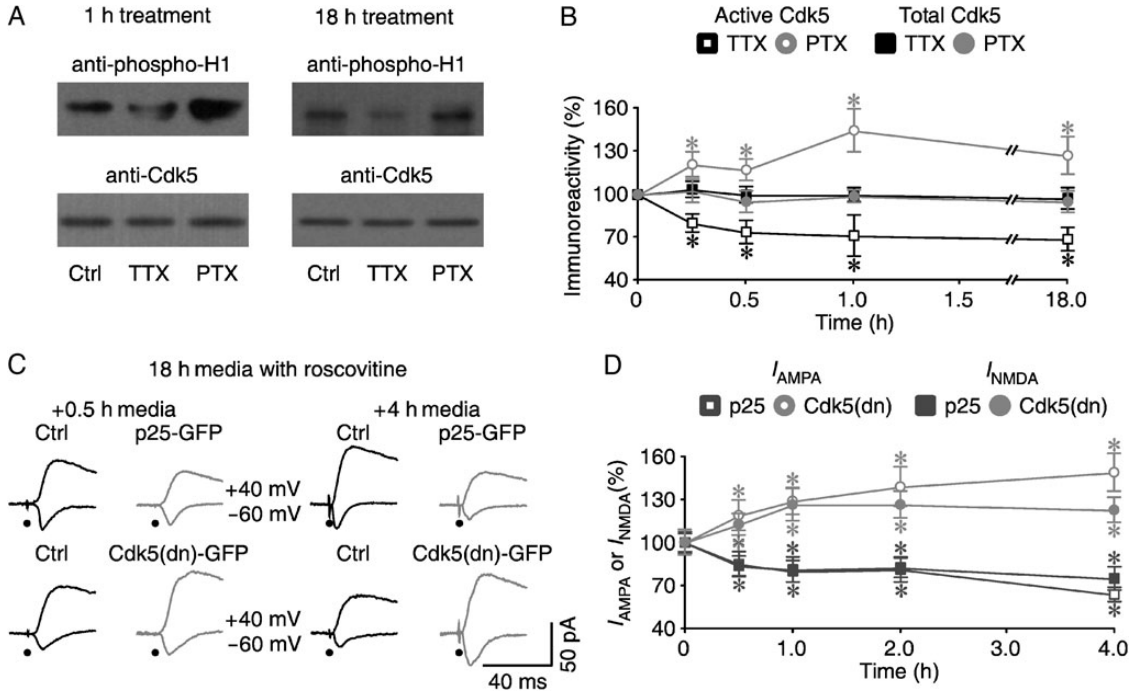

Figure 2. Cdk5 signals a novel rapid homeostatic regulation at synapses. (*A*) Blots of phosphorylated histone H1 and total Cdk5 in CA1 tissues cultured in normal media, media containing 2 µM TTX, or media containing 20 µM PTX for 1 or 18 h. (*B*) Relative levels of Cdk5 kinase activity measured using histone H1 as the substrate after 15 min (TTX: 80.5 ± 6.2%; $n = 12$; $P < 0.05$; PTX: 121.4 ± 8.8%; $n = 12$; $P < 0.05$; Wilcoxon tests compared with Ctrl: 100.0 ± 7.1%; $n = 12$), 30 min (TTX: 74.1 ± 8.3%; $n = 12$; $P < 0.01$; PTX: 117.5 ± 7.2%; $n = 12$; $P < 0.05$; Wilcoxon tests compared with Ctrl: 100.0 ± 9.0%; $n = 12$), 1 h (TTX: 71.6 ± 14.1%; $n = 12$; $P < 0.05$; PTX: 144.8 ± 15.4%; $n = 12$; $P < 0.05$; Wilcoxon tests compared with Ctrl: 100.0 ± 11.4%; $n = 12$), or 18 h (TTX: 68.5 ± 8.2%; $n = 12$; $P < 0.05$; PTX: 128.0 ± 12.9%; $n = 12$; $P < 0.05$; Wilcoxon tests compared with Ctrl: 100.0 ± 14.3%; $n = 12$) and total Cdk5 after 15 min (TTX: 103.2 ± 5.7%; $n = 12$; $P = 0.43$; PTX: 102.8 ± 8.1%; $n = 12$; $P = 0.43$ Wilcoxon tests compared with Ctrl: 100.0 ± 6.0%; $n = 12$), 30 min (TTX: 100.5 ± 5.9%; $n = 12$; $P = 0.58$; PTX: 95.2 ± 7.4%; $n = 12$; $P = 0.48$ Wilcoxon tests compared with Ctrl: 100.0 ± 5.6%; $n = 12$), 1 h (TTX: 100.3 ± 5.3%; $n = 12$; $P = 0.64$; PTX: 98.1 ± 4.2%; $n = 12$; $P = 0.70$ Wilcoxon tests compared with Ctrl: 100.0 ± 3.1%; $n = 12$), or 18 h (TTX: 97.5 ± 7.0%; $n = 12$; $P = 0.70$; PTX: 95.5 ± 7.6%; $n = 12$; $P = 0.39$ Wilcoxon tests compared with Ctrl: 100.0 ± 7.1%; $n = 12$) after TTX or PTX treatment. For each set of CA1 tissue cell lysates, 100 µg protein was used to IP Cdk5 and perform the kinase activity assay, and 20–40 µg protein was used to blot total Cdk5. The relative values and standard errors were normalized to average amounts of phos-H1 or total Cdk5 of CA1 cells cultured in normal media. (*C*) Evoked AMPA-R- (−60 mV) and NMDA-R- (+40 mV) mediated responses recorded from neighboring nonexpressing (Ctrl) and p25-GFP (upper) or Cdk5(dn)-GFP (lower) expressing cells cultured in media containing 25 µM roscovitine for 18 h followed by normal media for 0.5 or 4 h. (*D*) Amplitudes of synaptic AMPA and NMDA responses in p25-GFP (upper) or Cdk5(dn)-GFP (lower) expressing cells cultured in media containing 25 µM roscovitine for 18 h followed by normal media for different times. Values for AMPA responses after cultured in normal media for 0.5 h (Ctrl: −29.5 ± 2.3 pA; Exp: −25.1 ± 2.5 pA; $n = 23$; $P < 0.05$ for p25-GFP; Ctrl: −20.9 ± 1.8 pA; Exp: −24.8 ± 2.3 pA; $n = 22$; $P < 0.05$ for Cdk5(dn)-GFP), 1 h (Ctrl: −30.6 ± 2.7 pA; Exp: −24.4 ± 2.3 pA; $n = 30$; $P < 0.05$ for p25-GFP; Ctrl: −19.4 ± 1.8 pA; Exp: −25.0 ± 1.8 pA; $n = 31$; $P < 0.05$ for Cdk5(dn)-GFP), 2 h (Ctrl: −21.8 ± 2.1 pA; Exp: −17.7 ± 1.8 pA; $n = 26$; $P < 0.05$ for p25-GFP; Ctrl: −20.3 ± 1.5 pA; Exp: −28.2 ± 2.8 pA; $n = 31$; $P < 0.05$ for Cdk5(dn)-GFP), and 4 h (Ctrl: −32.5 ± 4.1 pA; Exp: −20.6 ± 1.7 pA; $n = 26$; $P < 0.05$ for p25-GFP; Ctrl: −22.1 ± 2.1 pA; Exp: −32.9 ± 2.9 pA; $n = 26$; $P < 0.005$ for Cdk5(dn)-GFP), and NMDA responses after cultured in normal media for 0.5 h (Ctrl: 70.1 ± 4.6 pA; Exp: 60.9 ± 5.0 pA; $n = 23$; $P < 0.01$ for p25-GFP; Ctrl: 61.3 ± 5.3 pA; Exp: 68.9 ± 4.7 pA; $n = 22$; $P < 0.01$ for Cdk5(dn)-GFP), 1 h (Ctrl: 69.8 ± 6.7 pA; Exp: 56.7 ± 6.2 pA; $n = 30$; $P < 0.05$ for p25-GFP; Ctrl: 52.9 ± 5.2 pA; Exp: 66.8 ± 6.0 pA; $n = 31$; $P < 0.05$ for Cdk5(dn)-GFP), 2 h (Ctrl: 44.0 ± 3.7 pA; Exp: 36.2 ± 3.0 pA; $n = 26$; $P < 0.05$ for p25-GFP; Ctrl: 43.2 ± 2.8 pA; Exp: 54.3 ± 4.2 pA; $n = 31$; $P < 0.05$ for Cdk5(dn)-GFP), and 4 h (Ctrl: 67.3 ± 6.2 pA; Exp: 50.1 ± 5.4 pA; $n = 26$; $P < 0.01$ for p25-GFP; Ctrl: 57.4 ± 5.5 pA; Exp: 70.4 ± 4.8 pA; $n = 26$; $P < 0.05$ for Cdk5(dn)-GFP). AMPA-R- and NMDA-R-mediated current amplitudes and standard errors were normalized to average values from control cells. Asterisks indicate $P < 0.05$ (Wilcoxon tests).

expressing Cdk5-targeting shRNAs had potentiated NMDA and AMPA responses (Fig. 1B,D). In contrast, neurons expressing scrambled shRNAs (S-shRNAs) had unaltered NMDA and AMPA responses (Fig. 1B,D). In addition, including roscovitine in cultured media occluded the shRNA-induced potentiation (Fig. 1D). Collectively, the dominant negative overexpression, shRNA knockdown and pharmacological inhibition experiments consistently support the idea that endogenous Cdk5 depresses glutamatergic transmission in CA1 neurons.

To determine whether activation of Cdk5 signaling requires synaptic activity, we incubated slices in high Mg^{2+} (12 mM) culture media, which depresses synaptic activity (Zhu et al. 2000). High Mg^{2+} occluded the potentiation induced by Cdk5(dn)-GFP or Cdk5-targeting shRNA (Fig. 1D–F), suggesting the involvement of synaptic activity in activation of Cdk5 signaling. To validate this finding, we included 2 μM TTX (which blocks Na^+ channels) or 20 μM PTX (which blocks $GABA_A$-Rs) in culture media to down- or up-regulate synaptic activity, respectively. In the presence of TTX, neurons expressing Cdk5(dn)-GFP had the same NMDA and AMPA responses as nearby nonexpressing neurons (Fig. 1E,F). This result suggests that blocking synaptic activity suppresses the depressive effects of endogenous Cdk5. In contrast, in the presence of PTX, neurons expressing Cdk5(dn)-GFP had enhanced potentiation compared with those cultured in normal media (Fig. 1E,F). This result suggests that enhancing synaptic activity augments the depressive effects of endogenous Cdk5. To further determine whether synaptic activity regulates Cdk5 signaling via activation of NMDA-Rs, we included 100 μM DL-APV, an NMDA-R blocker, in culture media. In the presence of 100 μM DL-APV, the Cdk5(dn)-GFP-induced potentiation of NMDA and AMPA responses were occluded with or without additional PTX in culture media (Fig. 1E,F), suggesting that activation of Cdk5 signaling requires synaptic NMDA-R activity. Together, these results indicate that Cdk5 serves as a regulator of homeostatic transmission at synapses, consistent with the previous reports (Seeburg et al. 2008; Kim and Ryan 2010; Mitra et al. 2011).

We then examined how synaptic activity regulates Cdk5 signaling by measuring the levels of Cdk5 kinase activity at different time points after PTX and TTX treatments. We found that TTX decreased and PTX increased Cdk5 kinase activity without affecting the total levels of Cdk5 (Fig. 2A,B). Interestingly, TTX and PTX rapidly altered Cdk5 kinase activity within 15 min, and the effects persisted for as long as 18 h (Fig. 2A,B). Because roscovitine can rapidly and reversibly pass through the membrane to inhibit Cdk5 (see Supplementary Fig. S4; see also Tomizawa et al. 2002; Yan et al. 2002), we decided to use the inhibitor as a tool to

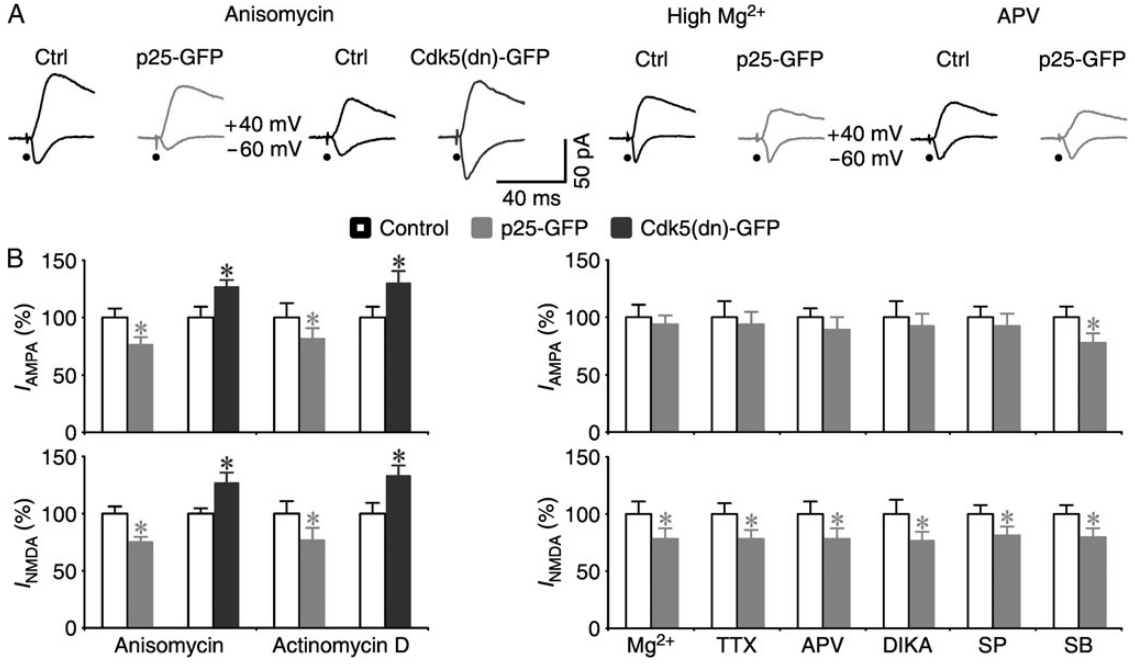

Figure 3. Cdk5 regulates synaptic homeostasis using a new signaling mechanism. (*A*) Evoked AMPA-R- (−60 mV) and NMDA-R- (+40 mV) mediated responses recorded from neighboring nonexpressing (Ctrl) and p25-GFP or Cdk5(dn)-GFP expressing cells cultured in media containing 25 μM roscovitine for 18 h followed by media containing 40 μM anisomycin for 4 h (upper) and neighboring nonexpressing (Ctrl) and p25-GFP expressing neurons cultured in 12 mM Mg^{2+} media or media with 100 μM DL-APV (lower). (*B*) (Left) Amplitudes of synaptic AMPA and NMDA responses in p25-GFP (upper) or Cdk5(dn)-GFP (lower) expressing neurons cultured in media containing 25 μM roscovitine for 18 h followed by media containing 40 μM anisomycin or 50 μM actinomycin D for 4 h. Values for AMPA responses in neurons treated with anisomycin (Ctrl: −23.5 ± 2.0 pA; Exp: −17.9 ± 1.6 pA; $n = 26$; $P < 0.05$ for p25-GFP; Ctrl: −19.3 ± 1.7 pA; Exp: −24.5 ± 1.2 pA; $n = 26$; $P < 0.05$ for Cdk5(dn)-GFP), or actinomycin D (Ctrl: −20.7 ± 2.5 pA; Exp: −16.7 ± 1.9 pA; $n = 22$; $P < 0.05$ for p25-GFP; Ctrl: −18.4 ± 1.8 pA; Exp: −23.8 ± 2.1 pA; $n = 22$; $P < 0.05$ for Cdk5(dn)-GFP), and NMDA responses in neurons treated with anisomycin (Ctrl: 64.2 ± 4.3 pA; Exp: 48.0 ± 3.6 pA; $n = 26$; $P < 0.005$ for p25-GFP; Ctrl: 52.1 ± 2.5 pA; Exp: 65.7 ± 4.8 pA; $n = 26$; $P < 0.05$ for Cdk5(dn)-GFP), or actinomycin D (Ctrl: 47.7 ± 5.4 pA; Exp: 36.6 ± 5.1 pA; $n = 22$; $P < 0.05$ for p25-GFP; Ctrl: 43.7 ± 4.4 pA; Exp: 58.2 ± 3.6 pA; $n = 22$; $P < 0.005$ for Cdk5(dn)-GFP). (Right) AMPA and NMDA responses in neurons expressing p25-GFP relative to neighboring nonexpressing control cells. Values for AMPA responses in p25-GFP expressing neurons cultured in media with 12 mM Mg^{2+} (Ctrl: −38.6 ± 4.4 pA; Exp: −36.0 ± 3.4 pA; $n = 30$; $P = 0.58$), 2 μM TTX (Ctrl: −31.6 ± 4.4 pA; Exp: −29.5 ± 3.4 pA; $n = 22$; $P = 0.78$), 100 μM DL-APV (Ctrl: −37.4 ± 3.0 pA; Exp: −33.3 ± 3.8 pA; $n = 28$; $P = 0.11$), 5 μM DCKA (Ctrl: −33.8 ± 4.7 pA; Exp: −31.0 ± 4.2 pA; $n = 20$; $P = 0.88$), 5 μM SP600125 (Ctrl: −31.1 ± 3.0 pA; Exp: −28.8 ± 3.0 pA; $n = 24$; $P = 0.44$), or 2 μM SB203580 (Ctrl: −32.6 ± 3.2 pA; Exp: −25.2 ± 2.8 pA; $n = 23$; $P < 0.05$), and values for NMDA responses in p25-GFP expressing neurons cultured in media with 12 mM Mg^{2+} (Ctrl: 67.1 ± 7.5 pA; Exp: 52.6 ± 5.8 pA; $n = 30$; $P < 0.05$), 2 μM TTX (Ctrl: 53.3 ± 5.2pA; Exp: 41.7 ± 3.8 pA; $n = 22$; $P = 0.75$), 100 μM DL-APV (Ctrl: 63.4 ± 7.0 pA; Exp: 49.5 ± 5.8 pA; $n = 28$; $P < 0.05$), 5 μM DCKA (Ctrl: 55.4 ± 6.8 pA; Exp: 42.4 ± 4.8 pA; $n = 20$; $P < 0.01$), 5 μM SP600125 (Ctrl: 52.9 ± 4.3 pA; Exp: 43.0 ± 4.3 pA; $n = 23$; $P < 0.05$) or 2 μM SB203580 (Ctrl: 52.9 ± 4.5 pA; Exp: 42.1 ± 4.2 pA; $n = 23$; $P < 0.05$). AMPA-R and NMDA-R mediated current amplitudes and standard errors were normalized to average values from control cells. Asterisks indicate $P < 0.05$ (Wilcoxon tests).

determine whether the altered Cdk5 activities had immediate impacts on synaptic transmission. We first expressed p25-GFP or Cdk5(dn)-GFP in CA1 neurons cultured in media containing roscovitine for 18 h (Fig. 2C,D), and then measured transmission at different times after removal of the inhibitor. Within 30 min after the removal of roscovitine (to remove the inhibition of Cdk5), neurons expressing p25-GFP and Cdk5(dn)-GFP had depressed and enhanced NMDA and AMPA responses, respectively (Fig. 2C,D). Together, these results showed that Cdk5 could be activated by synaptic activity within ~15 min and in turn depressed transmission within ~30 min. Because all known homeostatic regulators take at least 1–2 h to execute homeostatic feedbacks on synaptic transmission (Turrigiano 2008), our results indicate that Cdk5 regulates a new rapid homeostatic mechanism at synapses.

We wished to further explore the properties of homeostatic regulation of Cdk5 signaling. Previously identified homeostatic regulators control synaptic transmission using transcription- and/or translation-dependent mechanisms, which take at least 1 h to initiate homeostatic responses (Turrigiano 2008). We found that neither the transcription inhibitor, actinomycin D, nor the translation inhibitor, anisomycin, blocked the p25-GFP-induced synaptic depression and Cdk5(dn)-GFP-induced synaptic potentiation (Fig. 3), suggesting a transcription- and translation-independent mechanism. The classic slow homeostatic regulators depress AMPA responses prior to NMDA responses (Hsieh et al. 2006; Rial Verde et al. 2006; Seeburg et al. 2008; Evers et al. 2010; Sun et al. 2013). On the other hand, the rapid action of Cdk5 makes it uncertain whether Cdk5 depresses AMPA responses first (Tomizawa et al. 2002; Yan et al. 2002; Chergui et al. 2004), or suppresses NMDA responses first (Hawasli et al. 2007; Plattner et al. 2014). We investigated the synaptic depressions induced by p25 overexpression (Fig. 3), which is expected to constitutively stimulates Cdk5 signaling in the absence of upstream signaling (Patrick et al. 1999). We found that including high Mg^{2+}, TTX, NMDA-R antagonists APV or DCKA in culture media, which blocks NMDA-R-dependent modification of AMPA transmission (Malinow and Malenka 2002; Stornetta and Zhu 2011; Huganir and Nicoll 2013), blocked the p25-induced depression in AMPA responses but not the depression in NMDA responses (Fig. 3). These results suggest that Cdk5 signaling depresses NMDA responses prior to AMPA responses. The same AMPA responses in expressing and nonexpressing neurons are also suggestive of no effect of postsynaptic Cdk5 signaling on presynaptic glutamate release. Finally, previously reported homeostatic regulators depress AMPA responses via a signaling process that is sensitive to p38MAPK inhibitor SB203580, but not JNK inhibitor SP600125 (Hsieh et al. 2006; Origlia et al. 2008; Li et al. 2011). In contrast, the p25-induced synaptic depression of AMPA responses was blocked by SP600125, but not by SB203580 (Fig. 3B). Collectively, the biochemical, electrophysiological, and pharmacological analyses reveal that Cdk5 signals a rapid homeostasis of synaptic transmission using a novel feedback mechanism, different from the slow homeostatic regulators in kinetics, signaling transduction pathways, and physiological consequences (Turrigiano 2008).

Chronic Cdk5 Signaling Dynamically Regulates Slow Homeostatic Regulators

The rapid kinetics of Cdk5 signaling suggest that chronic stimulation of Cdk5 signaling should suppress production of slow homeostatic regulators (e.g., Aβ and Arc) by depressing synaptic activity (Turrigiano 2008). Yet, previous studies have shown that chronic hyperactivation of Cdk5 stimulates production of Aβ via a slow transcription-dependent process (Cruz et al. 2006; Wen et al. 2008). To resolve the apparent contradiction, we measured the protein levels of Aβ and Arc after 1–7 days of p25 overexpression. Western blot analysis revealed that overexpression of p25 in CA1 cells induced an initial decrease, followed by an increase in Aβ and Arc production that surpassed the baseline (Fig. 4). We further examined the effect of overexpression of p25 on the levels of extracellular Aβ, which is crucial for synaptic depression and synapse loss (Hsieh et al. 2006; Wen et al. 2008). Enzyme linked immunosorbent assay (ELISA) measurement showed that the levels of released Aβ in the culture media followed the same time course (Fig. 4C). Moreover, the culture media induced the Aβ-like effects on transmission following

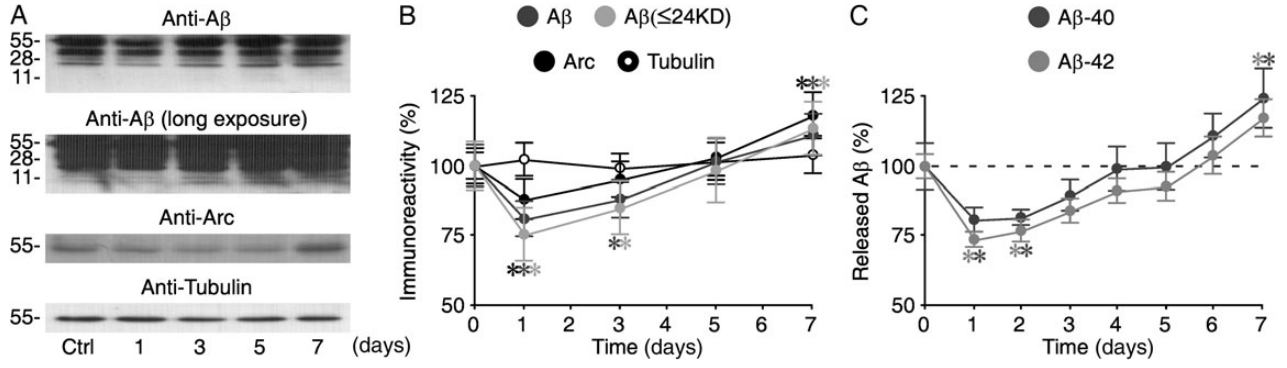

Figure 4. Chronic overproduction of p25 dynamically regulates Aβ and Arc signaling. (*A*) Expression of Aβ, Arc and tubulin after 1-, 3-, 5-, and 7-day overexpression of p25 in CA1 cells. Note the relatively weak bands of low-order Aβ oligomers (≤24 kDa) appeared after a longer exposure time, reflecting presumably the reduced retention of low molecular weight proteins by the standard membrane used in the experiment, and all bands detected by anti-rat Aβ have the same time course. (*B*) Relative amounts of Aβ (1-day: 80.7 ± 6.1, $n = 15$, $P < 0.005$; 3-day: 88.2 ± 6.9%, $n = 15$, $P < 0.05$; 5-day: 101.5 ± 8.2, $n = 15$; $P = 0.87$; 7-day: 111.2 ± 7.2, $n = 15$; $P < 0.05$; Wilcoxon tests compared with Ctrl: 100.0 ± 7.3%, $n = 15$), low-order Aβ oligomers (1-day: 75.1 ± 9.5, $n = 12$, $P < 0.005$; 3-day: 85.0 ± 9.6%, $n = 12$, $P < 0.05$; 5-day: 97.8 ± 11.1, $n = 12$; $P = 0.75$; 7-day: 113.4 ± 9.6, $n = 12$; $P < 0.05$; Wilcoxon tests compared with Ctrl (0-day): 100.0 ± 8.8%, $n = 12$), Arc (1-day: 88.1 ± 7.1, $n = 18$, $P < 0.005$; 3-day: 94.7 ± 6.4%, $n = 18$, $P = 0.15$; 5-day: 103.0 ± 6.6, $n = 18$; $P = 0.27$; 7-day: 117.7 ± 8.2, $n = 18$; $P < 0.05$ Wilcoxon tests compared with Ctrl (0-day): 100.0 ± 6.2%, $n = 18$), and tubulin (1-day: 101.7 ± 6.0, $n = 25$, $P = 0.48$; 3-day: 98.6 ± 5.3%, $n = 25$, $P = 0.62$; 5-day: 101.4 ± 6.7, $n = 25$; $P = 0.54$; 7-day: 103.3 ± 6.6, $n = 25$; $P = 0.99$; Wilcoxon tests compared with Ctrl (0-day): 100.0 ± 4.8%, $n = 25$) in p25-expressing cells compared with control nonexpressing CA1 cells. Each lane was loaded with 45 μg hippocampal CA1 cell lysate protein. (*C*) Relative levels of released Aβ-40 (1-day: 255.3 ± 20.8 pM, $n = 11$, $P < 0.005$; 2-day: 255.8 ± 11.7 pM, $n = 11$, $P < 0.05$; 3-day: 293.5 ± 25.5 pM, $n = 11$; $P = 0.16$; 4-day: 336.1 ± 36.8 pM, $n = 11$; $P = 0.93$; 5-day: 339.9 ± 37.7 pM, $n = 11$; $P = 0.86$; 6-day: 389.0 ± 35.9 pM, $n = 11$; $P = 0.18$; 7-day: 448.4 ± 49.3 pM, $n = 11$; $P < 0.05$; Wilcoxon tests compared with Ctrl (0-day): 337.7 ± 39.0 pM, $n = 11$), and Aβ-42 (1-day: 28.3 ± 1.7 pM, $n = 11$, $P < 0.005$; 2-day: 30.5 ± 2.6 pM, $n = 11$, $P < 0.01$; 3-day: 36.0 ± 2.8 pM, $n = 11$; $P = 0.06$; 4-day: 41.0 ± 2.7 pM, $n = 11$; $P = 0.11$; 5-day: 42.6 ± 3.3 pM, $n = 11$; $P = 0.29$; 6-day: 50.6 ± 4.4 pM, $n = 11$; $P = 0.99$; 7-day: 61.3 ± 4.4 pM, $n = 11$; $P < 0.05$; Wilcoxon tests compared with Ctrl (0-day): 47.6 ± 2.5 pM, $n = 11$) in culture media after 1–7 days of overexpression of p25 in CA1 cells in cultured slices. Asterisks indicate $P < 0.05$.

the same time course (see Supplementary Fig. S5; cf. Hsieh et al. 2006; Wen et al. 2008). These results confirm that the chronic overproduction p25 dynamically regulates Aβ production. Together, these results suggest a notion that the p25-stimulated Cdk5 signaling initially inhibits the slow homeostatic regulator signaling via suppressing synaptic activity, and later enhances the slow homeostatic regulator signaling via stimulating transcription, which reconciles the previous seemingly contradictory findings (Cruz et al. 2006; Turrigiano 2008; Wen et al. 2008).

The above mentioned analysis suggests that Cdk5 signaling is mediated by JNK signaling (see Fig. 3B), which controls depotentiation (Zhu et al. 2005; Yang et al. 2011). In contrast, Aβ/Arc signaling is mediated by p38MAPK signaling (Hsieh et al. 2006; Origlia et al. 2008; Li et al. 2011), which controls LTD (Hsieh et al. 2006; Rial Verde et al. 2006). Thus, we reasoned that prolonged overproduction of p25 may modulate the signaling mechanisms of both JNK-mediated depotentiation and p38MAPK-mediated LTD. To dissect p25-mediated effects on the signaling mechanisms, we first measured synaptic plasticity after overexpression of p25-GFP for 16 h, which had not yet produced a significant change in transmission or production of Aβ and Arc (Fig. 5A,B). Neurons overexpressing p25 for 16 h had reduced LTP, but unaltered LTD (Fig. 5C). To determine whether overexpression of p25 actually reduces LTP and/or enhances depotentiation, we measured depotentiation in p25-expressing neurons. SB203580 was included in the bath solution in this experiment to prevent induction of LTD (Zhu et al. 2005). We found that in addition to the progressive loss of potentiation after LTP induction, neurons expressing p25 had reduced synaptic depression after application of the depotentiation stimuli (Fig. 5C), which is suggestive of constitutively enhanced depotentiation signaling (cf. see Zhu et al. 2005). To confirm this idea, we measured LTP again in the bath solution containing additional SP600125, which blocks depotentiation (Zhu et al. 2005; Yang et al. 2011). In the presence of SP600125, p25-expressing neurons had the same LTP as nonexpressing neurons (Fig. 5C). These results suggest that activating Cdk5 signaling by acute overexpression of p25 selectively enhances the signaling mechanism

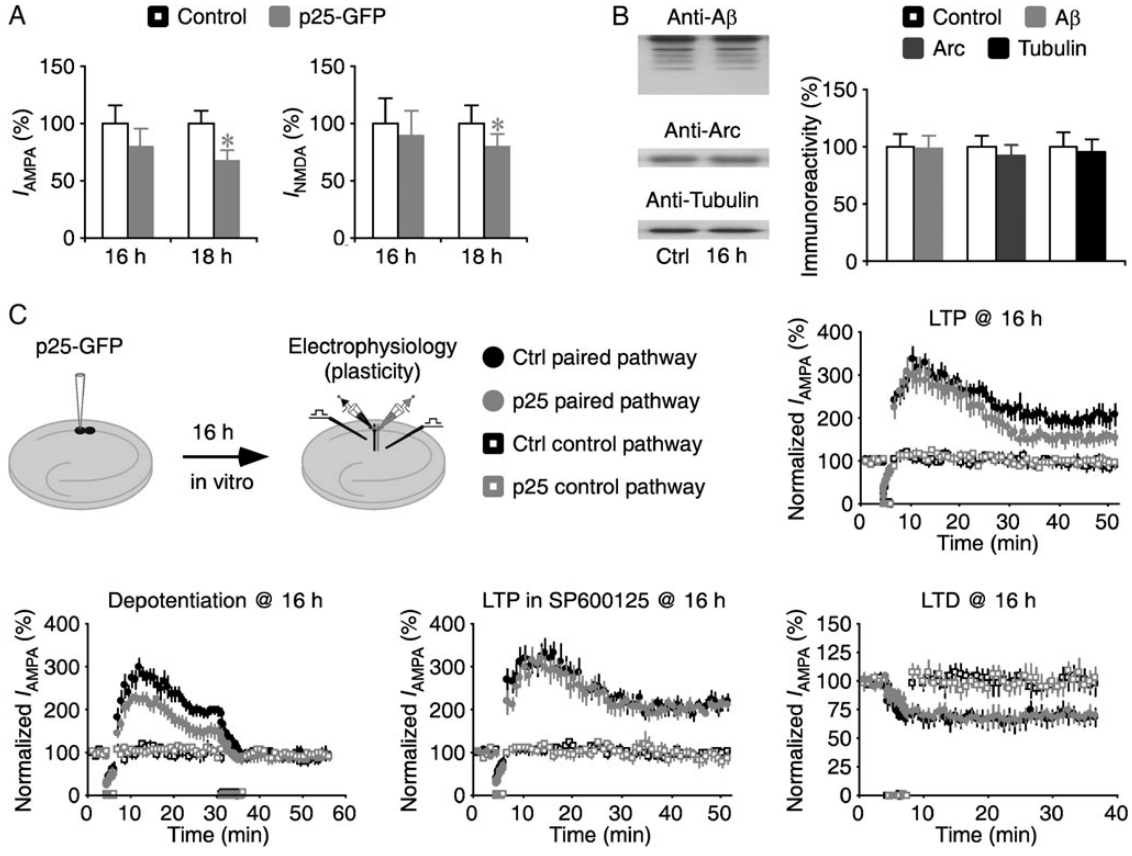

Figure 5. Acute overproduction of p25 stimulates depotentiation. (*A*) Overexpression of p25-GFP for 18 h, but not 16 h, induced significant depressions in AMPA and NMDA responses in p25-GFP expressing neurons. Values for AMPA (Ctrl: −21.5 ± 3.5 pA; Exp: −17.2 ± 3.3 pA; $n = 20$; $P = 0.28$) and NMDA (Ctrl: 62.0 ± 13.7 pA; Exp: 55.6 ± 12.9 pA; $n = 20$; $P = 0.79$) responses in neurons after 16-h overexpression of p25-GFP (see Fig. 1C for the values for those after 18 h of overexpression of p25-GFP). Note no significant difference in the relative depressions after 16 and 18 h of overexpression of p25-GFP (16-h: 20.0%; 18-h: 33.4%; $P = 0.21$; Mann–Whitney Rank Sum test). AMPA-R and NMDA-R mediated current amplitudes and standard errors were normalized to average values from control cells. (*B*) (Left) Expression of Aβ, Arc and tubulin after 16-h overexpression of p25 in CA1 cells. (Right) Relative amounts of Aβ (Ctrl: 100.0 ± 10.7%; 16-h: 98.5 ± 11.1; $n = 14$, $P = 0.71$), Arc (Ctrl: 100.0 ± 8.7%; 16-h: 92.5 ± 8.6; $n = 14$, $P = 0.33$), and tubulin (Ctrl: 100.0 ± 12.6%; 16-h: 95.0 ± 11.1; $n = 14$, $P = 0.88$) in p25-expressing cells compared with control nonexpressing CA1 cells. (*C*) (Upper left) Schematic drawing outlines in vitro plasticity experimental design. Relative LTP, depotentiation, LTP in SP600125, and LTD in expressing neurons compared with control nonexpressing neurons after 16-h overexpression of p25. Values for the potentiation and depression between control nonexpressing neurons and p25-expressing neurons in LTP (Ctrl: 199.0 ± 15.7%; Exp: 154.1 ± 11.9%; $n = 18$; $P < 0.005$ for paired pathways; Ctrl: 94.2 ± 8.6%; Exp: 97.5 ± 5.6%; $n = 18$; $P = 0.93$ for control pathways), depotentiation (Ctrl: 99.3 ± 7.4%; Exp: 59.9 ± 10.6%; $n = 14$; $P < 0.05$ for paired pathways; Ctrl: 96.3 ± 5.1%; Exp: 93.2 ± 6.3%; $n = 14$; $P = 0.78$ for control pathways), LTP in SP600125 (Ctrl: 207.3 ± 10.2%; Exp: 204.1 ± 9.7%; $n = 14$; $P = 0.88$ for paired pathways; Ctrl: 95.3 ± 11.5%; Exp: 98.1 ± 4.8%; $n = 14$; $P = 0.55$ for control pathways), and LTD (Ctrl: 68.3 ± 5.0%; Exp: 69.8 ± 4.2%; $n = 18$; $P = 0.74$ for paired pathways; Ctrl: 100.4 ± 3.4%; Exp: 100.8 ± 4.1%; $n = 18$; $P = 0.65$ for control pathways) after 16-h overexpression of p25. Asterisks indicate $P < 0.05$ (Wilcoxon tests).

of JNK-mediated depotentiation without affecting the signaling mechanisms of LTP and LTD.

We then examined the effects of chronic overexpression of p25 on the signaling mechanisms of LTP, depotentiation and LTD (Fig. 6). We measured synaptic plasticity after overexpression of p25-GFP for 2 days, at which time the protein levels of Aβ and Arc had a significant reduction. Neurons overexpressing p25 for 2 days had reduced LTP, unaltered LTP in the presence of additional SP600125, enhanced depotentiation, and reduced LTD (Fig. 6*B–E*). These results suggest that chronic overproduction of

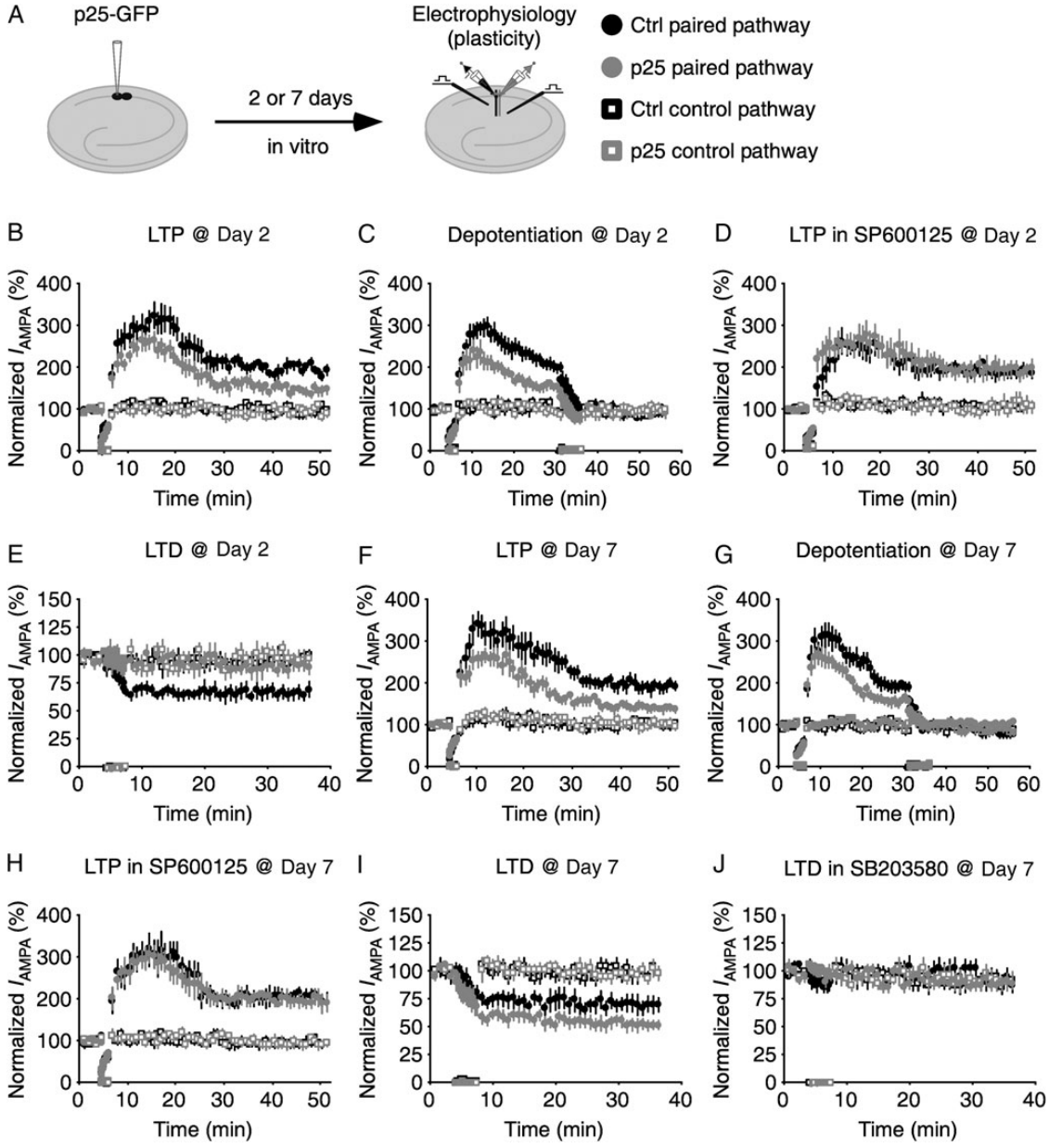

Figure 6. Chronic overproduction of p25 stimulates depotentiation and dynamically regulates LTD. (*A*) Schematic drawing outlines in vitro plasticity experimental design. (*B–E*) Relative LTP, depotentiation, LTP in SP600125, and LTD in expressing neurons compared with control nonexpressing neurons after 2-day overexpression of p25. Values for the potentiation and depression in control nonexpressing neurons and p25-expressing neurons in LTP (Ctrl: 198.9 ± 4.6%; Exp: 150.9 ± 8.2%; $n = 17$; $P < 0.005$ for paired pathways; Ctrl: 95.3 ± 5.4%; Exp: 98.9 ± 4.4%; $n = 17$; $P = 0.55$ for control pathways), depotentiation (Ctrl: 109.0 ± 10.7%; Exp: 57.4 ± 6.4%; $n = 14$; $P < 0.05$ for paired pathways; Ctrl: 97.4 ± 4.9%; Exp: 93.8 ± 4.4%; $n = 14$; $P = 0.47$ for control pathways), LTP in SP600125 (Ctrl: 206.3 ± 10.4%; Exp: 208.3 ± 12.8%; $n = 15$; $P = 0.96$ for paired pathways; Ctrl: 89.9 ± 13.0%; Exp: 95.2 ± 3.3%; $n = 15$; $P = 0.46$ for control pathways), and LTD (Ctrl: 68.1 ± 4.3%; Exp: 93.6 ± 3.8%; $n = 17$; $P < 0.005$ for paired pathways; Ctrl: 97.1 ± 3.9%; Exp: 95.4 ± 4.9%; $n = 17$; $P = 0.88$ for control pathways) after 2-day overexpression of p25. (*F–J*) Relative LTP, depotentiation, LTP in SP600125, and LTD in expressing neurons compared with control nonexpressing neurons after 7-day overexpression of p25. Values for the potentiation and depression in control nonexpressing neurons and p25-expressing neurons in LTP (Ctrl: 195.1 ± 9.0%; Exp: 142.3 ± 5.9%; $n = 18$; $P < 0.005$ for paired pathways; Ctrl: 102.9 ± 8.3%; Exp: 100.2 ± 4.3%; $n = 18$; $P = 0.90$ for control pathways), depotentiation (Ctrl: 103.8 ± 10.7%; Exp: 54.9 ± 7.9%; $n = 14$; $P < 0.01$ for paired pathways; Ctrl: 92.1 ± 4.8%; Exp: 96.0 ± 4.8%; $n = 14$; $P = 0.22$ for control pathways), LTP in SP600125 (Ctrl: 205.3 ± 9.0%; Exp: 199.2 ± 8.3%; $n = 13$; $P = 0.55$ for paired pathways; Ctrl: 92.3 ± 5.4%; Exp: 95.4 ± 3.5%; $n = 13$; $P = 0.51$ for control pathways), LTD (Ctrl: 72.2 ± 5.4%; Exp: 55.8 ± 3.9%; $n = 17$; $P < 0.005$ for paired pathways; Ctrl: 100.3 ± 2.9%; Exp: 100.0 ± 3.2%; $n = 17$; $P = 0.91$ for control pathways), and LTD with additional SB203580 (Ctrl: 97.0 ± 5.9%; Exp: 92.9 ± 2.9%; $n = 16$; $P = 0.47$ for paired pathways; Ctrl: 94.1 ± 3.3%; Exp: 94.5 ± 3.6%; $n = 16$; $P = 0.68$ for control pathways) after 7-day overexpression of p25.

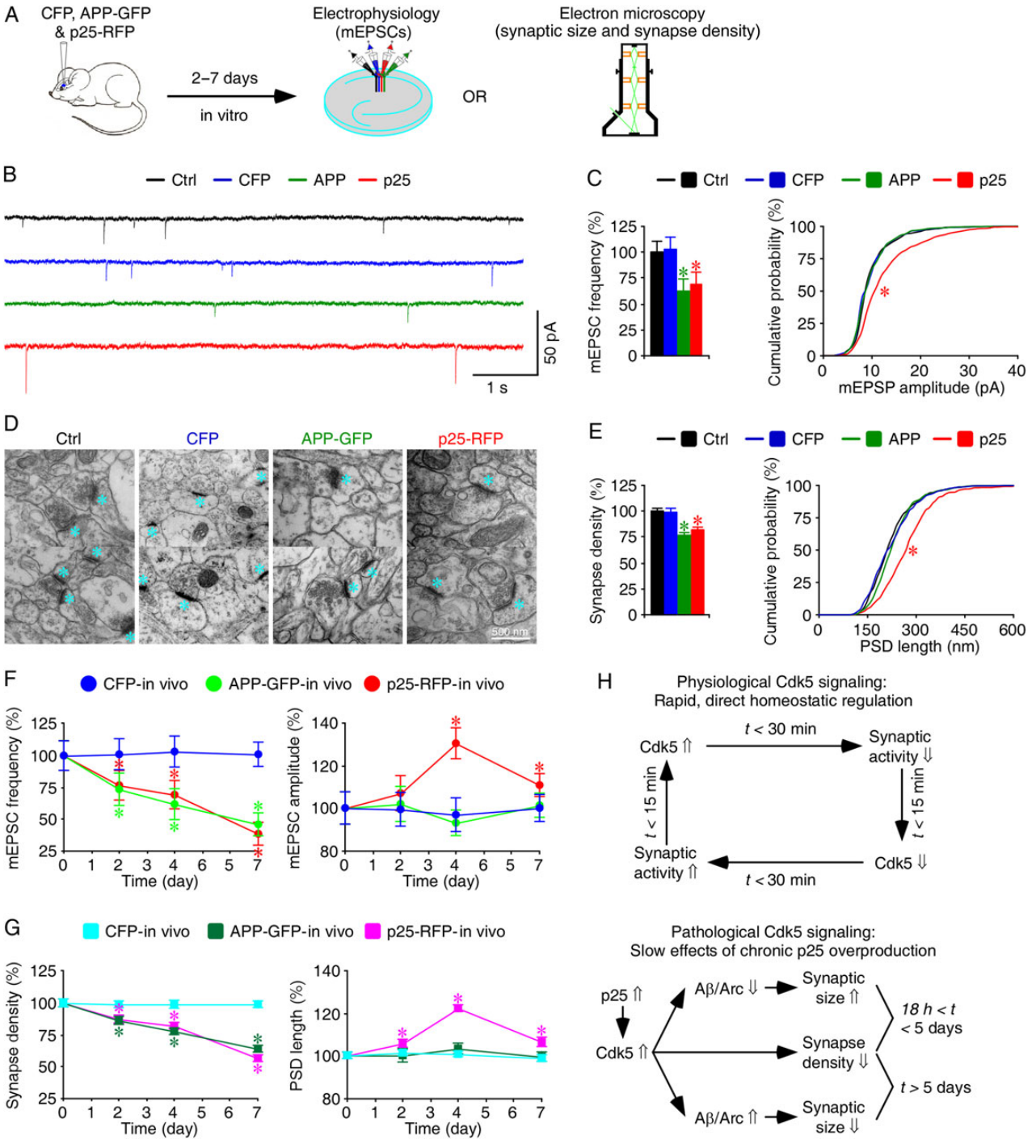

Figure 7. Chronic overproduction of p25 induces Alzheimer-like synaptic alterations in intact brains. (*A*) Schematic drawing outlines in vivo experimental design. (*B*) Miniature EPSCs recorded simultaneously from nearby control nonexpressing CA1 neurons, CA1 neurons overexpressing CFP, APP-GFP, or p25-RFP in acute slices after 4 days of in vivo expression. (*C*) Average mEPSC frequencies of control nonexpressing CA1 neurons, CA1 neurons overexpressing CFP, APP-GFP, or p25-RFP (left), and cumulative distributions of mEPSC amplitudes of control nonexpressing CA1 neurons, CA1 neurons overexpressing CFP, APP-GFP, or p25-RFP (right) after 4 days of in vivo expression. (*D*) Electron microscopic images from hippocampal CA1 stratum radiatum regions of control rats, rats overexpressing CFP, APP-GFP, or p25-RFP after 4 days of in vivo expression. Cyan asterisks indicate individual synapses. (*E*) Average synaptic densities of control nonexpressing CA1 tissues, CA1 tissues overexpressing CFP, p25-RFP, or APP-GFP (left), and cumulative distributions of PSD lengths of control nonexpressing CA1 tissues, CA1 tissues overexpressing CFP, APP-GFP, or p25-RFP (right) after 4 days of in vivo expression. (*F*) (Left) Relative mEPSC frequency in control nonexpressing CA1 neurons, CA1 neurons overexpressing CFP, APP-GFP, or p25-RFP at different expression time. Value for the average mEPSC frequency of each neuron group after 2-day (CFP: 0.44 ± 0.05 Hz, $n = 20$, $P = 0.77$; APP: 0.32 ± 0.06 Hz, $n = 20$, $P < 0.01$; p25: 0.33 ± 0.05 Hz, $n = 20$, $P < 0.05$; Wilcoxon tests compared with Ctrl: 0.44 ± 0.05 Hz, $n = 20$), 4-day (CFP: 0.50 ± 0.06 Hz, $n = 17$, $P = 0.62$; APP: 0.30 ± 0.06 Hz, $n = 17$, $P < 0.005$; p25: 0.34 ± 0.05 Hz, $n = 17$, $P < 0.05$; Wilcoxon tests compared with Ctrl: 0.49 ± 0.05 Hz, $n = 17$), and 7-day (CFP: 0.59 ± 0.06 Hz, $n = 18$, $P = 0.95$; APP: 0.27 ± 0.05 Hz, $n = 18$, $P < 0.01$; p25: 0.23 ± 0.05 Hz, $n = 18$, $P < 0.005$; Wilcoxon tests compared with Ctrl: 0.59 ± 0.06 Hz, $n = 18$) in vivo overexpression. (Right) Relative mEPSC amplitude in control nonexpressing CA1 neurons, CA1 neurons overexpressing CFP, APP-GFP, or p25-RFP at different expression time. Values for the average mEPSC amplitude of each neuron group after 2-day (CFP: 9.21 ± 0.70 pA, $n = 20$, $P = 0.94$; APP: 9.44 ± 0.77 pA, $n = 20$, $P = 0.85$; p25: 9.88 ± 0.75 pA, $n = 20$, $P = 0.19$; Wilcoxon tests compared with Ctrl:

p25 initially enhances the signaling mechanism of depotentiation and suppresses the signaling mechanism of LTD. Moreover, we measured synaptic plasticity after overexpression of p25-GFP for 7 days, at which time the protein levels of Aβ and Arc had a significant increase. Neurons overexpressing p25 for 7 days had reduced LTP, unaltered LTP in the presence of additional SP600125, enhanced depotentiation and enhanced LTD (Fig. 6*F–I*). Finally, including the bath solution SB203580, which inhibits the Aβ and Arc downstream signaling effector p38MAPK (Hsieh et al. 2006; Rial Verde et al. 2006), blocked the enhanced LTD in neurons overexpressing p25 (Fig. 6*J*). These results suggest that prolonged overexpression of p25 enhances the signaling mechanisms of Cdk5–JNK-mediated depotentiation and p38MAPK-mediated LTD. Collectively, the biochemical, ELISA, and synaptic plasticity assessments all suggest that chronic stimulation of Cdk5 signaling constitutively stimulates the signaling mechanism of JNK-mediated depotentiation and dynamically regulates the signaling mechanism of Aβ/Arc–p38MAPK-mediated LTD.

We speculated that Cdk5 signaling may induce complex changes in synapse density and synaptic size since it could alter both JNK- and p38MAPK-mediated signaling mechanisms. To test this idea, we examined in CA1 neurons expressing Rap2-GFP and/or Rap1-RFP (see Supplementary Fig. S6A), which can modulate JNK and p38MAPK signaling, respectively (Zhu et al. 2002, 2005; Huang et al. 2004; Machida et al. 2004; Kielland et al. 2009). We measured frequency and amplitude of mEPSCs, indicators of synaptic synapse density and synaptic size, respectively. Neurons expressing Rap2(wt)-GFP alone, which stimulates JNK signaling (Zhu et al. 2005; Kielland et al. 2009), had reduced mEPSC frequency but unaltered mEPSC amplitude (see Supplementary Fig. S6B,C). These results suggest that acute overproduction of p25 may reduce synapse density without affecting synaptic size. In contrast, neurons coexpressing Rap2(wt)-GFP and Rap1(dn)-RFP, which stimulate JNK signaling and suppress p38MAPK signaling, respectively (Zhu et al. 2002, 2005; Kielland et al. 2009), had slightly reduced mEPSC frequency but considerably increased mEPSC amplitude (see Supplementary Fig. S6D,E). Moreover, neurons coexpressing Rap2(wt)-GFP and Rap1(wt)-RFP, which stimulate JNK signaling and p38MAPK signaling, respectively (Zhu et al. 2002, 2005; Kielland et al. 2009), had reduced mEPSC frequency and amplitude (see Supplementary Fig. S6F, G). These results suggest that simultaneously enhancing Cdk5–JNK signaling and suppressing Aβ/Arc–p38MAPK signaling induces the concurrent reduction in synapse density and increase in synaptic size, whereas simultaneously enhancing Cdk5–JNK signaling and Aβ/Arc–p38MAPK signaling induces concomitant reduction in synapse density and synaptic size.

Chronic Overproduction of p25 Induces the Alzheimer-Like Pathology

We were intrigued by the finding that simultaneously enhancing Cdk5–JNK signaling and suppressing Aβ/Arc–p38MAPK signaling can induce the concurrent reduction in synapse density and increase in synaptic size, the characteristic early Alzheimer-like synaptic pathology (Davies et al. 1987; Bertoni-Freddari et al. 1990; DeKosky and Scheff 1990). To determine whether chronic overproduction of p25, seen in Alzheimer's brain (Cruz and Tsai 2004), may induce the Alzheimer-like synaptic pathology, we examined synaptic effects of overexpression of p25 in CA1 neurons in cultured slices (see Supplementary Fig. S7) and intact brain (Fig. 7*A–G*) for up to 7 days. We first made functional assessment of the synaptic changes with electrophysiological recordings of mEPSCs, and then validated the results with direct ultrastructural measurements of synapse density and synaptic size. At Day 2, electrophysiology recordings revealed that p25-expressing neurons had significantly reduced (by ~25%) mEPSCs frequency but slightly increased (by ~5%) mEPSCs amplitude. Correspondingly, electron microscopic images showed that p25-expressing neurons had reduced synapse density but enhanced synaptic size. These results are consistent with an overall Cdk5-mediated synaptic depression. By Day 4, expression of p25 induced a small additional reduction (~5%) in mEPSCs frequency but a large increase (~25%) in mEPSCs amplitude, which were associated with the same changes in synapse density and synaptic size. These results are consistent with the engagement of Aβ- and Arc-mediated homeostatic regulation by day 4. At Day 7, expression of p25 began to reduce both mEPSCs frequency (by ~35%) and amplitude (by ~20%) rapidly, which were mirrored by the changes in synapse density and synaptic size as well, consistent with the involvement of the unified action of Cdk5, Aβ, and Arc signaling in synaptic depression. As controls, we found that overexpression of GFP (see Supplementary Fig. S7) or CFP (Fig. 7*B–G*) alone had no effects on mEPSCs frequency and amplitude, and synapse density and synaptic size during the same period. As an additional control, we also overexpressed GFP-tagged amyloid precursor protein (APP) that overproduces Aβ (Kamenetz et al. 2003; Hsieh et al. 2006), in CA1 neurons in intact brains. Overexpression of APP progressively reduced mEPSCs frequency and synapse density, but had no effect on mEPSCs amplitude and

9.23 ± 0.69 pA, $n = 20$), 4-day (CFP: 8.82 ± 0.72 pA, $n = 17$, $P = 0.65$; APP: 8.48 ± 0.55 pA, $n = 17$, $P = 0.41$; p25: 12.64 ± 0.81 pA, $n = 17$, $P < 0.005$; Wilcoxon tests Ctrl: 9.07 ± 0.50 pA, $n = 17$), and 7-day (CFP: 9.46 ± 0.59 pA, $n = 18$, $P = 0.91$; APP: 9.57 ± 0.55 pA, $n = 18$, $P = 0.40$; p25: 10.45 ± 0.49 pA, $n = 18$, $P < 0.05$; Wilcoxon tests compared with Ctrl: 9.45 ± 0.62 pA, $n = 18$) in vivo overexpression. (*G*) (Left) Relative synapse density in control nonexpressing CA1 neurons, CA1 neurons overexpressing CFP, APP-GFP, or p25-RFP at different expression time. Values for the average synapse density, counted as synapses per 100 μm^2, after 2-day (CFP: 12.4 ± 0.4, $n = 50$ ultrathin sections from 8 animals, $P = 0.59$; APP: 10.7 ± 0.4; $n = 49$ ultrathin sections from 8 animals, $P < 0.005$; p25: 10.9 ± 0.4, $n = 50$ ultrathin sections from 8 animals, $P < 0.005$; Mann–Whitney Rank Sum tests compared with Ctrl: 12.5 ± 0.4, $n = 50$ from 8 animals), 4-day (CFP: 12.4 ± 0.4, $n = 50$ ultrathin sections from 8 animals, $P = 0.71$; APP: 9.7 ± 0.3; $n = 50$ ultrathin sections from 9 animals, $P < 0.001$; p25: 10.2 ± 0.3, $n = 50$ ultrathin sections from 9 animals, $P < 0.001$; Mann–Whitney Rank Sum tests compared with Ctrl: 12.5 ± 0.4, $n = 50$ ultrathin sections from 9 animals), and 7-day (CFP: 12.5 ± 0.3, $n = 50$ ultrathin sections from 8 animals, $P = 0.89$; APP: 8.1 ± 0.3; $n = 50$ ultrathin sections from 8 animals, $P < 0.001$; p25: 7.2 ± 0.3, $n = 50$ ultrathin sections from 8 animals, $P < 0.001$; Mann–Whitney Rank Sum tests compared with Ctrl: 12.7 ± 0.4, $n = 50$ from 8 animals) in vivo overexpression. (Right) Relative PSD length in control nonexpressing CA1 neurons, CA1 neurons overexpressing CFP, p25-RFP, or APP-GFP at different expression time. Values for the average PSD length of each group after 2-day (CFP: 228.3 ± 3.3 nm, $n = 619$ synapses from 8 animals, $P = 0.81$; APP: 225.7 ± 4.0 nm, $n = 526$ synapses from 8 animals, $P = 0.80$; p25: 238.4 ± 3.9 nm, $n = 545$ synapses from 8 animals, $P < 0.01$; Mann–Whitney Rank Sum tests compared with Ctrl: 225.2 ± 3.5 nm, $n = 625$ from 8 animals), 4-day (CFP: 224.2 ± 2.9 nm, $n = 616$ synapses from 8 animals, $P = 0.85$; APP: 230.4 ± 2.9 nm, $n = 484$ synapses from 9 animals, $P = 0.07$; p25: 272.7 ± 3.0 nm, $n = 510$ synapses from 9 animals, $P < 0.001$; Mann–Whitney Rank Sum tests compared with Ctrl: 222.9 ± 2.7 nm, $n = 626$ synapses from 9 animals), and 7-day (CFP: 226.7 ± 3.7 nm, $n = 623$ synapses from 8 animals, $P = 0.90$; APP: 227.9 ± 4.7 nm, $n = 407$ synapses from 8 animals, $P = 0.73$; p25: 244.9 ± 5.0 nm, $n = 361$ synapses from 8 animals, $P < 0.005$; Mann–Whitney Rank Sum tests compared with Ctrl: 229.4 ± 4.3 nm, $n = 595$ from 8 animals) in vivo overexpression. The relative values and standard errors were normalized to average mEPSC frequency, amplitude, synapse density, and PSD length from control cells. Note the significantly more reductions in mEPSC frequency and synapse density in p25-expressing CA1 neurons compared with APP-expressing neurons after 7-day overexpression. Asterisks indicate $P < 0.05$. (*H*) A schematic model describes physiological and pathological Cdk5 signaling.

synaptic size during the same 7-day period (Fig. 7*B*–*G*), consistent with previous reports (Sun et al. 2009; Wei et al. 2010). Collectively, these results suggest that chronic overproduction of p25 induces the characteristic Alzheimer-like synaptic pathology.

Discussion

In this study, we have investigated the properties and function of Cdk5 signaling at hippocampal CA1 synapses. Our investigation reveals that Cdk5 signals a novel, rapid form of homeostasis of synaptic transmission (Fig. 7*H*). Our analysis also reveals that chronic overproduction of p25 can induce the concurrent alterations in synapse density and synaptic size characteristic of the early Alzheimer-like synaptic pathology (Fig. 7*H*).

Physiological Cdk5 Signaling

We report here that Cdk5 signals synaptic depression via a homeostatic synaptic mechanism (Fig. 7*H*), consistent with previous reports (Seeburg et al. 2008; Kim and Ryan 2010; Mitra et al. 2011). Our data suggests that Cdk5 can rapidly depress NMDA and AMPA responses, using a transcription- and translation-independent mechanism, and that Cdk5 depresses transmission via a kinase mechanism (Chergui et al. 2004; Peng et al. 2013). Interestingly, Cdk5 reacts quickly (within ~15 min) in response to altered synaptic transmission. In fact, Cdk5 can respond and execute homeostatic regulation to preserve homeostatic transmission within ~15–30 min; thus, the kinetics of Cdk5 signaling are far faster than previously characterized homeostatic regulators that take from 1–12 h to react and produce a response (Turrigiano 2008). It is known that Hebbian synaptic plasticity can change transmission strength within ~15 min (Stornetta and Zhu 2011), and unbalanced transmission may induce destructive status epilepticus within 1–2 h (Fountain and Lothman 1995; Rakhade and Jensen 2009). The rapid Cdk5 homeostatic signaling provides an explanation for the long-standing conundrum of how neurons may preserve homeostasis intermediately after Hebbian synaptic plasticity to avoid status epilepticus.

Pathological Cdk5 Signaling

Our results suggest that chronic stimulation of Cdk5 signaling by overproduction of p25 enhances JNK signaling and dynamically regulates production of Aβ and Arc. Initially, overproduction of p25 stimulates JNK signaling, which depresses synaptic transmission and reduces synapse density by removing the newly delivered synaptic AMPA-Rs (Zhu et al. 2005; Kielland et al. 2009; Nadif Kasri et al. 2009). This initial synaptic depression is expected to cause homeostatic suppression of production of Aβ and Arc (Turrigiano 2008). The reduced Aβ and Arc signaling, which controls synaptic removal of AMPA-Rs from the existing synapses (Hsieh et al. 2006; Rial Verde et al. 2006), should thus result in an increase in the size of the residual synapses. In contrast, the prolonged overproduction of p25 stimulates Aβ and Arc production, presumably via a slower, more powerful transcription-dependent mechanism (Cruz et al. 2006; Wen et al. 2008). Together, the up-regulated JNK- and Aβ/Arc-mediated synaptic depressions can work in unison to depress and eliminate synapses.

Previous electron microscopic analysis identifies the concurrent reduction in synapse density and increase in synaptic size to be a pathological hallmark of Alzheimer's disease (DeKosky and Scheff 1990; Scheff and Price 2006; Scheff et al. 2006). Our electrophysiological and ultrastructural analyses show that chronic overexpression of p25 induces a concurrent reduction in synapse density and increase in synaptic size (Fig. 7*H*). These results lead us to conclude that p25 is a molecule capable of inducing the hallmark early Alzheimer-like synaptic pathology. This finding is also supported by additional lines of evidence. For example, direct measurement of the level of p25 shows multiple-fold increases in p25 accumulation in Alzheimer's brains (Patrick et al. 1999; Tseng et al. 2002; Swatton et al. 2004), although no significant change (Taniguchi et al. 2001; Tandon et al. 2003) and even a reduction (Engmann et al. 2011) in p25 expression in human patients have also been reported. The differences reported in these studies are likely to result from the technical difficulty in postmortem preservation of p25 (Cruz and Tsai 2004). Nevertheless, the marked enhancement in Cdk5 activity and Cdk5-mediated specific phosphorylation are consistently observed at all stages of Alzheimer's disease (Lee et al. 1999; Swatton et al. 2004; Cole et al. 2007). Moreover, overproduction of p25 alters both JNK- and Aβ/Arc–p38MAPK-mediated synaptic depressions, consistent with the apparently normal ERK signaling, but aberrant JNK and p38MAPK activities in the early Alzheimer's brains (Ferrer et al. 2005; Stornetta and Zhu 2011). Furthermore, the prolonged overproduction of p25 dynamically regulates production of Aβ and Arc. This is congruent with the recent observations made with the improved indicators and/or imaging techniques that the high expressions of Aβ and Arc are only seen during the late stages of Alzheimer's disease, with reduced and unchanged (rather than increased) levels of Aβ and Arc observed in human brains prior to these stages (Ingelsson et al. 2004; Jack et al. 2010; Gomar et al. 2011; Wu et al. 2011). Finally, overproduction of p25 pushes the regulation of synaptic Cdk5 and Aβ/Arc signaling away from their "happy-medium" dynamic ranges (i.e., being either too low to achieve proper activation or too high to stay away from saturation at synapses), which decreases the capacity for synaptic plasticity (McCormack et al. 2006), and impairs cognition (Costa and Silva 2003; Thomas and Huganir 2004; Stornetta and Zhu 2011). This can explain why both decreased synapse density and increased synaptic size are correlated with cognitive impairment during the preclinical and early stages of Alzheimer's disease (DeKosky and Scheff 1990; Scheff and Price 2006). These findings also predict that the transient, subtle change in synaptic signaling might enhance selective form(s) of plasticity and/or learning, while the prolonged, prominent alternation in synaptic signaling would inevitably deviate the "happy-medium" signaling and impair the overall plasticity and cognition, as observed for Cdk5 signaling (Fischer et al. 2005; Plattner et al. 2014). Consistent with the previous reports (Sun et al. 2009; Wei et al. 2010), our electrophysiological and electron microscopic data suggest that overproduction of Aβ reduces synapse density and synaptic size. These results support a view that overproduction of Aβ alone may not be sufficient to initiate the early Alzheimer-like concurrent reduction in synapse density and increase in synaptic size. Instead, our analysis suggests that Aβ contributes to initially the increase in synaptic size and later the persistent synapse elimination during the general disease development process. Obviously, Aβ, if validated, may still be the primary cause of the synaptic pathology of ~1–2% of patients with early onset familial Alzheimer's disease (Selkoe 2012). To the best of our knowledge, our results provide the very first evidence that links Cdk5 signaling to the early pathogenesis of the majority of Alzheimer's cases. Therefore, there is a good reason to hope that our new findings will inspire more research and perhaps also development of testable models for the early pathogenesis of the disease.

Supplementary Material

Supplementary Material can be found at http://www.cercor.oxfordjournals.org.

Funding

This study is supported in part by a research collaboration Award from the National Natural Science Foundation of China (Y.S. and J.J.Z.), a postdoctoral fellowship from the Alzheimer's and Related Diseases Research Award Fund (L.Z.), the Harrison Faculty Undergraduate Advisor Award (J.J.Z.), the Howard Hughes Medical Institute (S.C.S. and L.-H.T.) and the US National Institutes of Health (L.-H.T. and J.J.Z.). This paper is the part of a dissertation in partial fulfillment of the requirements of the BS degree (Y.S.) at the Peking University.

Notes

We thank Dr Steve DeKosky for inspirational discussions, Drs Yu Xiang and Weifeng Xu for invaluable technical advice, and members of the Zhu laboratory for comments and technical assistance. *Conflict of Interest:* None declared.

References

Arendt T. 2009. Synaptic degeneration in Alzheimer's disease. Acta Neuropathol. 118:167–179.

Bertoni-Freddari C, Fattoretti P, Casoli T, Meier-Ruge W, Ulrich J. 1990. Morphological adaptive response of the synaptic junctional zones in the human dentate gyrus during aging and Alzheimer's disease. Brain Res. 517:69–75.

Chergui K, Svenningsson P, Greengard P. 2004. Cyclin-dependent kinase 5 regulates dopaminergic and glutamatergic transmission in the striatum. Proc Natl Acad Sci U S A. 101:2191–2196.

Cheung ZH, Ip NY. 2012. Cdk5: a multifaceted kinase in neurodegenerative diseases. Trends Cell Biol. 22:169–175.

Cole AR, Noble W, van Aalten L, Plattner F, Meimaridou R, Hogan D, Taylor M, LaFrancois J, Gunn-Moore F, Verkhratsky A, et al. 2007. Collapsin response mediator protein-2 hyperphosphorylation is an early event in Alzheimer's disease progression. J Neurochem. 103:1132–1144.

Costa RM, Silva AJ. 2003. Mouse models of neurofibromatosis type I: bridging the GAP. Trends Mol Med. 9:19–23.

Cruz JC, Kim D, Moy LY, Dobbin MM, Sun X, Bronson RT, Tsai LH. 2006. p25/cyclin-dependent kinase 5 induces production and intraneuronal accumulation of amyloid beta in vivo. J Neurosci. 26:10536–10541.

Cruz JC, Tsai LH. 2004. Cdk5 deregulation in the pathogenesis of Alzheimer's disease. Trends Mol Med. 10:452–458.

Davies CA, Mann DM, Sumpter PQ, Yates PO. 1987. A quantitative morphometric analysis of the neuronal and synaptic content of the frontal and temporal cortex in patients with Alzheimer's disease. J Neurol Sci. 78:151–164.

DeKosky ST, Marek K. 2003. Looking backward to move forward: early detection of neurodegenerative disorders. Science. 302:830–834.

DeKosky ST, Scheff SW. 1990. Synapse loss in frontal cortex biopsies in Alzheimer's disease: correlation with cognitive severity. Ann Neurol. 27:457–464.

Engmann O, Hortobagyi T, Thompson AJ, Guadagno J, Troakes C, Soriano S, Al-Sarraj S, Kim Y, Giese KP. 2011. Cyclin-dependent kinase 5 activator p25 is generated during memory formation and is reduced at an early stage in Alzheimer's disease. Biol Psychiatry. 70:159–168.

Evers DM, Matta JA, Hoe HS, Zarkowsky D, Lee SH, Isaac JT, Pak DT. 2010. Plk2 attachment to NSF induces homeostatic removal of GluA2 during chronic overexcitation. Nat Neurosci. 13:1199–1207.

Ferrer I, Gomez-Isla T, Puig B, Freixes M, Ribe E, Dalfo E, Avila J. 2005. Current advances on different kinases involved in tau phosphorylation, and implications in Alzheimer's disease and tauopathies. Curr Alzheimer Res. 2:3–18.

Fischer A, Sananbenesi F, Pang PT, Lu B, Tsai LH. 2005. Opposing roles of transient and prolonged expression of p25 in synaptic plasticity and hippocampus-dependent memory. Neuron. 48:825–838.

Fountain NB, Lothman EW. 1995. Pathophysiology of status epilepticus. J Clin Neurophysiol. 12:326–342.

Gomar JJ, Bobes-Bascaran MT, Conejero-Goldberg C, Davies P, Goldberg TE. 2011. Utility of combinations of biomarkers, cognitive markers, and risk factors to predict conversion from mild cognitive impairment to Alzheimer disease in patients in the Alzheimer's disease neuroimaging initiative. Arch Gen Psychiatry. 68:961–969.

Guerreiro RJ, Gustafson DR, Hardy J. 2012. The genetic architecture of Alzheimer's disease: beyond APP, PSENs and APOE. Neurobiol Aging. 33:437–456.

Hawasli AH, Benavides DR, Nguyen C, Kansy JW, Hayashi K, Chambon P, Greengard P, Powell CM, Cooper DC, Bibb JA. 2007. Cyclin-dependent kinase 5 governs learning and synaptic plasticity via control of NMDAR degradation. Nat Neurosci. 10:880–886.

Hsieh H, Boehm J, Sato C, Iwatsubo T, Tomita T, Sisodia S, Malinow R. 2006. AMPAR removal underlies Abeta-induced synaptic depression and dendritic spine loss. Neuron. 52:831–843.

Hu H, Qin Y, Bochorishvili G, Zhu Y, van Aelst L, Zhu JJ. 2008. Ras signaling mechanisms underlying impaired GluR1-dependent plasticity associated with fragile X syndrome. J Neurosci. 28:7847–7862.

Huang CC, You JL, Wu MY, Hsu KS. 2004. Rap1-induced p38 mitogen-activated protein kinase activation facilitates AMPA receptor trafficking via the GDI.Rab5 complex. Potential role in (S)-3,5-dihydroxyphenylglycene-induced long term depression. J Biol Chem. 279:12286–12292.

Huganir RL, Nicoll RA. 2013. AMPARs and synaptic plasticity: the last 25 years. Neuron. 80:704–717.

Ingelsson M, Fukumoto H, Newell KL, Growdon JH, Hedley-Whyte ET, Frosch MP, Albert MS, Hyman BT, Irizarry MC. 2004. Early Abeta accumulation and progressive synaptic loss, gliosis, and tangle formation in AD brain. Neurology. 62:925–931.

Jack CR Jr, Wiste HJ, Vemuri P, Weigand SD, Senjem ML, Zeng G, Bernstein MA, Gunter JL, Pankratz VS, Aisen PS, et al. 2010. Brain beta-amyloid measures and magnetic resonance imaging atrophy both predict time-to-progression from mild cognitive impairment to Alzheimer's disease. Brain. 133:3336–3348.

Jiang X, Wang G, Lee AJ, Stornetta RL, Zhu JJ. 2013. The organization of two new cortical interneuronal circuits. Nat Neurosci. 16:210–218.

Kamenetz F, Tomita T, Hsieh H, Seabrook G, Borchelt D, Iwatsubo T, Sisodia S, Malinow R. 2003. APP processing and synaptic function. Neuron. 37:925–937.

Kielland A, Bochorishvili G, Corson J, Zhang L, Rosin DL, Heggelund P, Zhu JJ. 2009. Activity patterns govern synapse-specific AMPA-R

trafficking between deliverable and synaptic pools. Neuron. 62:84–101.

Kim SH, Ryan TA. 2010. CDK5 serves as a major control point in neurotransmitter release. Neuron. 67:797–809.

Lee AJ, Wang G, Jiang X, Johnson SM, Hoang ET, Lante F, Stornetta RL, Beenhakker MP, Shen Y, Zhu J. 2015. Canonical organization of layer 1 neuron-led cortical inhibitory and disinhibitory interneuronal circuits. Cereb Cortex. 25:2114–2126.

Lee KY, Clark AW, Rosales JL, Chapman K, Fung T, Johnston RN. 1999. Elevated neuronal Cdc2-like kinase activity in the Alzheimer disease brain. Neurosci Res. 34:21–29.

Li S, Jin M, Koeglsperger T, Shepardson NE, Shankar GM, Selkoe DJ. 2011. Soluble Abeta oligomers inhibit long-term potentiation through a mechanism involving excessive activation of extrasynaptic NR2B-containing NMDA receptors. J Neurosci. 31:6627–6638.

Lim CS, Hoang ET, Viar KE, Stornetta RL, Scott MM, Zhu JJ. 2014. Pharmacological rescue of Ras signaling, GluA1-dependent synaptic plasticity, and learning deficits in a fragile X model. Genes Dev. 28:273–289.

Liu F, Ma XH, Ule J, Bibb JA, Nishi A, DeMaggio AJ, Yan Z, Nairn AC, Greengard P. 2001. Regulation of cyclin-dependent kinase 5 and casein kinase 1 by metabotropic glutamate receptors. Proc Natl Acad Sci U S A. 98:11062–11068.

Machida N, Umikawa M, Takei K, Sakima N, Myagmar BE, Taira K, Uezato H, Ogawa Y, Kariya K. 2004. Mitogen-activated protein kinase kinase kinase kinase 4 as a putative effector of Rap2 to activate the c-Jun N-terminal kinase. J Biol Chem. 279: 15711–15714.

Malinow R, Malenka RC. 2002. AMPA receptor trafficking and synaptic plasticity. Annu Rev Neurosci. 25:103–126.

McCormack SG, Stornetta RL, Zhu JJ. 2006. Synaptic AMPA receptor exchange maintains bidirectional plasticity. Neuron. 50:75–88.

Mitra A, Mitra SS, Tsien RW. 2011. Heterogeneous reallocation of presynaptic efficacy in recurrent excitatory circuits adapting to inactivity. Nat Neurosci. 15:250–257.

Myers KR, Wang G, Sheng Y, Conger KK, Casanova JE, Zhu JJ. 2012. Arf6-GEF BRAG1 regulates JNK-mediated synaptic removal of GluA1-containing AMPA receptors: a new mechanism for nonsyndromic X-linked mental disorder. J Neurosci. 32: 11716–11726.

Nadif Kasri N, Nakano-Kobayashi A, Malinow R, Li B, Van Aelst L. 2009. The Rho-linked mental retardation protein oligophrenin-1 controls synapse maturation and plasticity by stabilizing AMPA receptors. Genes Dev. 23:1289–1302.

Origlia N, Righi M, Capsoni S, Cattaneo A, Fang F, Stern DM, Chen JX, Schmidt AM, Arancio O, Yan SD, et al. 2008. Receptor for advanced glycation end product-dependent activation of p38 mitogen-activated protein kinase contributes to amyloid-beta-mediated cortical synaptic dysfunction. J Neurosci. 28:3521–3530.

Patrick GN, Zukerberg L, Nikolic M, de la Monte S, Dikkes P, Tsai LH. 1999. Conversion of p35 to p25 deregulates Cdk5 activity and promotes neurodegeneration. Nature. 402: 615–622.

Peng YR, Hou ZH, Yu X. 2013. The kinase activity of EphA4 mediates homeostatic scaling-down of synaptic strength via activation of Cdk5. Neuropharmacology. 65:232–243.

Plattner F, Hernandez A, Kistler TM, Pozo K, Zhong P, Yuen EY, Tan C, Hawasli AH, Cooke SF, Nishi A, et al. 2014. Memory enhancement by targeting Cdk5 regulation of NR2B. Neuron. 81:1070–1083.

Qin Y, Zhu Y, Baumgart JP, Stornetta RL, Seidenman K, Mack V, van Aelst L, Zhu JJ. 2005. State-dependent Ras signaling and AMPA receptor trafficking. Genes Dev. 19:2000–2015.

Rakhade SN, Jensen FE. 2009. Epileptogenesis in the immature brain: emerging mechanisms. Nat Rev Neurol. 5:380–391.

Reisberg B, Shulman MB, Torossian C, Leng L, Zhu W. 2010. Outcome over seven years of healthy adults with and without subjective cognitive impairment. Alzheimer's Dementia. 6:11–24.

Rial Verde EM, Lee-Osbourne J, Worley PF, Malinow R, Cline HT. 2006. Increased expression of the immediate-early gene arc/arg3.1 reduces AMPA receptor-mediated synaptic transmission. Neuron. 52:461–474.

Scheff SW, Price DA. 2006. Alzheimer's disease-related alterations in synaptic density: neocortex and hippocampus. J Alzheimer's Dis. 9:101–115.

Scheff SW, Price DA, Schmitt FA, Mufson EJ. 2006. Hippocampal synaptic loss in early Alzheimer's disease and mild cognitive impairment. Neurobiol Aging. 27:1372–1384.

Seeburg DP, Feliu-Mojer M, Gaiottino J, Pak DT, Sheng M. 2008. Critical role of CDK5 and Polo-like kinase 2 in homeostatic synaptic plasticity during elevated activity. Neuron. 58: 571–583.

Selkoe DJ. 2012. Preventing Alzheimer's disease. Science. 337: 1488–1492.

Seo J, Giusti-Rodriguez P, Zhou Y, Rudenko A, Cho S, Ota KT, Park C, Patzke H, Madabhushi R, Pan L, et al. 2014. Activity-dependent p25 generation regulates synaptic plasticity and Abeta-induced cognitive impairment. Cell. 157:486–498.

Sharma P, Sharma M, Amin ND, Albers RW, Pant HC. 1999. Regulation of cyclin-dependent kinase 5 catalytic activity by phosphorylation. Proc Natl Acad Sci U S A. 96:11156–11160.

Sheng M, Sabatini BL, Sudhof TC. 2012. Synapses and Alzheimer's disease. Cold Spring Harb Perspect Biol. 4:1–18.

Stornetta RL, Zhu JJ. 2011. Ras and Rap signaling in synaptic plasticity and mental disorders. Neuroscientist. 17:54–78.

Su SC, Tsai LH. 2011. Cyclin-dependent kinases in brain development and disease. Annu Rev Cell Dev Biol. 27:465–491.

Sun B, Halabisky B, Zhou Y, Palop JJ, Yu G, Mucke L, Gan L. 2009. Imbalance between GABAergic and glutamatergic transmission impairs adult neurogenesis in an animal model of Alzheimer's disease. Cell Stem Cell. 5:624–633.

Sun H, Kosaras B, Klein PM, Jensen FE. 2013. Mammalian target of rapamycin complex 1 activation negatively regulates Polo-like kinase 2-mediated homeostatic compensation following neonatal seizures. Proc Natl Acad Sci U S A. 110:5199–5204.

Swatton JE, Sellers LA, Faull RL, Holland A, Iritani S, Bahn S. 2004. Increased MAP kinase activity in Alzheimer's and Down syndrome but not in schizophrenia human brain. Eur J Neurosci. 19:2711–2719.

Tandon A, Yu H, Wang L, Rogaeva E, Sato C, Chishti MA, Kawarai T, Hasegawa H, Chen F, Davies P, et al. 2003. Brain levels of CDK5 activator p25 are not increased in Alzheimer's or other neurodegenerative diseases with neurofibrillary tangles. J Neurochem. 86:572–581.

Taniguchi S, Fujita Y, Hayashi S, Kakita A, Takahashi H, Murayama S, Saido TC, Hisanaga S, Iwatsubo T, Hasegawa M. 2001. Calpain-mediated degradation of p35 to p25 in postmortem human and rat brains. FEBS Lett. 489:46–50.

Thomas GM, Huganir RL. 2004. MAPK cascade signalling and synaptic plasticity. Nat Rev Neurosci. 5:173–183.

Tomizawa K, Ohta J, Matsushita M, Moriwaki A, Li ST, Takei K, Matsui H. 2002. Cdk5/p35 regulates neurotransmitter release

through phosphorylation and downregulation of P/Q-type voltage-dependent calcium channel activity. J Neurosci. 22:2590–2597.

Tsai LH, Takahashi T, Caviness VS Jr, Harlow E. 1993. Activity and expression pattern of cyclin-dependent kinase 5 in the embryonic mouse nervous system. Development. 119:1029–1040.

Tseng HC, Zhou Y, Shen Y, Tsai LH. 2002. A survey of Cdk5 activator p35 and p25 levels in Alzheimer's disease brains. FEBS Lett. 523:58–62.

Turrigiano GG. 2008. The self-tuning neuron: synaptic scaling of excitatory synapses. Cell. 135:422–435.

Wang G, Wyskiel DR, Yang W, Wang Y, Milbern LC, Lalanne T, Jiang X, Shen Y, Sun Q-Q, Zhu JJ. 2015. An optogenetics- and imaging-assisted simultaneous multiple patch-clamp recordings system for decoding complex neural circuits. Nat Protoc. 10:397–412.

Wei W, Nguyen LN, Kessels HW, Hagiwara H, Sisodia S, Malinow R. 2010. Amyloid beta from axons and dendrites reduces local spine number and plasticity. Nat Neurosci. 13:190–196.

Wen Y, Yu WH, Maloney B, Bailey J, Ma J, Marie I, Maurin T, Wang L, Figueroa H, Herman M, et al. 2008. Transcriptional Regulation of beta-secretase by p25/cdk5 leads to enhanced amyloidogenic processing. Neuron. 57:680–690.

Wu J, Petralia RS, Kurushima H, Patel H, Jung MY, Volk L, Chowdhury S, Shepherd JD, Dehoff M, Li Y, et al. 2011. Arc/Arg3.1 regulates an endosomal pathway essential for activity-dependent beta-amyloid generation. Cell. 147:615–628.

Yan Z, Chi P, Bibb JA, Ryan TA, Greengard P. 2002. Roscovitine: a novel regulator of P/Q-type calcium channels and transmitter release in central neurons. J Physiol. 540:761–770.

Yang H, Courtney MJ, Martinsson P, Manahan-Vaughan D. 2011. Hippocampal long-term depression is enhanced, depotentiation is inhibited and long-term potentiation is unaffected by the application of a selective c-Jun N-terminal kinase inhibitor to freely behaving rats. Eur J Neurosci. 33:1647–1655.

Zhu JJ, Esteban JA, Hayashi Y, Malinow R. 2000. Postnatal synaptic potentiation: delivery of GluR4-containing AMPA receptors by spontaneous activity. Nat Neurosci. 3:1098–1106.

Zhu JJ, Qin Y, Zhao M, Van Aelst L, Malinow R. 2002. Ras and Rap control AMPA receptor trafficking during synaptic plasticity. Cell. 110:443–455.

Zhu Y, Pak D, Qin Y, McCormack SG, Kim MJ, Baumgart JP, Velamoor V, Auberson YP, Osten P, van Aelst L, et al. 2005. Rap2-JNK removes synaptic AMPA receptors during depotentiation. Neuron. 46:905–916.